Journal of Thermal Analysis and Calorimetry (2019) 135:437–460
https://doi.org/10.1007/s10973-018-7070-9

Combination of nanofluid and inserts for heat transfer enhancement

Gaps and challenges

S. Rashidi[1] · M. Eskandarian[2] · O. Mahian[3] · S. Poncet[4]

Received: 13 January 2018 / Accepted: 10 February 2018 / Published online: 23 February 2018

Abstract
Improving heat transfer is a critical subject for energy conservation systems which directly affects economic efficiency of these systems. There are active and passive methods which can be employed to enhance the rate of heat transfer without reducing the general efficiency of the energy conservation systems. Among these methods, passive techniques are more cost-effective and reliable in comparison with active ones as they have no moving parts. To achieve further improvements in heat transfer performances, some researchers combined passive techniques. This article performs a review of the literature on the area of heat transfer improvement employing a combination of nanofluid and inserts. Inserts are baffles, twisted tape, vortex generators, and wire coil inserts. The progress made and the current challenges for each combined system are discussed, and some conclusions and suggestions are made for future research.

Keywords Heat transfer enhancement · Passive techniques · Nanofluid · Inserts

List of symbols

d, D	Inner diameter of tube (m)
d_p	Nanoparticle diameter (nm)
D_h	Hydraulic diameter (m)
e	Wire diameter (m)
e_l	Winglets–length ratio (-)
e_p	Winglets–pitch ratio (-)
e_w	Winglets–width ratio (-)
f	Friction factor (-)
h	Twist tape pitch (m)
H	Pitch of twisted tape (m)
I_p	Longitudinal pitch (m)
l	Twist length (m)
L	Duct length (m)
N	Number of tapes (-)
Nu	Nusselt number (-)
p	Pitch ratio (-)
p	Perimeter of tube (m)
p	Power (W)
Pr	Prandtl number (-)
Re	Reynolds number (-)
S	Tube surface (m^2)
T	Tape thickness (m)
t_p	Transverse pitch (m)
w	Tape width (m)
w_h	Wing height (m)
w_w	Wing width (m)
y	Twist length (m)
Y	Twist ratio (-)
y_o	Overlapped pitch length of tape (m)
x	Axial distance (m)

Subscripts/superscripts

f	Base fluid
m	Bulk
nf	Nanofluid
p	Particle
TA	Twisted tape with alternate axis

✉ S. Poncet
Sebastien.Poncet@usherbrooke.ca

[1] Department of Mechanical Engineering, Ferdowsi University of Mashhad, Mashhad 91775-1111, Iran

[2] Department of Mechanical Engineering, Semnan University, P.O. Box: 35196-45399, Semnan, Iran

[3] Fluid Mechanics, Thermal Engineering and Multiphase Flow Research Laboratory (FUTURE Lab.), Department of Mechanical Engineering, Faculty of Engineering, King Mongkut's University of Technology Thonburi, Bangmod, Bangkok 10140, Thailand

[4] Department of Mechanical Engineering, Université de Sherbrooke, Sherbrooke, QC J1K 2R1, Canada

TT Typical twisted tape

Greek symbols

α Wing attach angle (°)
α_f Area modification factor (°)
β Wing attack angle (°)
μ Dynamic viscosity (kg m^{-1} s^{-1})
φ Solid volume fraction of nanoparticles (-)

Abbreviations

CNT	Carbon nanotube
DW	Delta wing
DWP	Delta winglet
HL	High to low
LH	Low to high
MWCNT	Multiwall carbon nanotubes
PEC	Performance evaluation criterion
RW	Rectangular wing
RWP	Rectangular winglet
U	Uniform

Introduction

Improving the heat transfer rate is one of the critical challenges in various industries containing electronic equipment, solar systems, chemical vapour deposition facilities, heat exchangers, and so on. It is necessary to remove the heat for avoiding the formation of hot spots which affect the lifespan of mechanical and electronic equipment and may lead to permanent damage. Accordingly, using an efficient cooling method is essential to disintegrate the thermal load on these devices and keep the peak efficiency in all situations.

There are active and passive techniques for improving heat transfer rate. An active technique employs an external source of energy to improve the heat transfer rate, while passive techniques employ no energy in this regard [1]. Generally, passive techniques are more affordable and reliable in comparison with active ones as they have no moving parts.

Researchers have already employed different passive techniques to enhance the heat transfer rate in different thermal devices. Some of these passive techniques apply rough surfaces [2], porous materials [3, 4], nanofluids [5, 6], corrugated surfaces [7, 8] or install turbulators or swirl flow tools [9, 10].

Some researchers reviewed the techniques for improving heat transfer rate in different systems. Kakaç and Pramuanjaroenkij [11] reviewed the potentials of nanofluids to improve the convective heat transfer. Their review indicated that more studies should be performed on the behaviour of nanofluids as a two-phase fluid because the slip velocity of the particles in the base liquid has a major influence on the heat transfer efficiency of nanofluids. Sundar and Singh [12] reviewed the correlations of nanofluid forced convection heat transfer and friction in a pipe with inserts for both the laminar and turbulent regimes. Their review only covers the papers published before 2012, while considerable activities in this field are performed after 2012. Their survey indicated that the significant numbers of the correlations were presented for spherical nanoparticles. Kareem et al. [13] reviewed heat transfer improvement due to corrugations and more especially to wavy tubes. They reported that helically coiled corrugated tubes have more heat transfer improvement as they have compound influences of curvatures and corrugations. Sheikholeslami et al. [14] reviewed potentials of swirl flow equipment for heat transfer improvement. They reported that wire coil has a superior overall efficiency when considering the pressure losses. Varun et al. [15] reviewed the activities performed on heat transfer improvement in twisted tape inserts. Their review showed that twisted tapes could be used in microfiltration of milk as they have a small value of pressure drop penalty. Che Sidik et al. [16] provided an overview of passive methods for heat transfer improvement in microchannel heat sink. They concluded that nanofluids as an alternative coolant technique could be used for improving the efficiency of microchannel heat sinks. Gallegos and Sharma [17] reviewed the potential of flexible plates as vortex generators for enhancing the heat transfer rate. They reported that very few experimental investigations had been performed to study the influences of flexible plate material parameters on their thermal improvement abilities. Mohammed et al. [18] reviewed activities performed for heat transfer improvement through facing step and wavy walls with and without nanofluids. They showed that the heat transfer improvement due to nanofluid in the facing step channel might achieve about 60%.

The heat transfer base liquids containing water, ethylene glycol, oil, propylene glycol, which are commonly employed in industry, have poor thermal characteristics. To overcome this deficiency, novel technologies are used to enhance the thermophysical characteristics of the conventional cooling liquids. One of these effective techniques consists of adding solid particles of nanosize with high thermal conductivity [19, 20]. In many applications, even more enhancement in heat transfer rate is favourable to meet the industry requirements for superior performance. Some attempts have been already made to combine various improvement techniques for enhancing the performance of thermal systems. Accordingly, some researchers employed simultaneously nanofluids and other passive techniques to achieve this goal. This article performs a review of the literature on the area of heat transfer improvement

employing a combination of nanofluid and inserts. This paper more focuses on the newer papers especially recent papers published after 2012. Inserts are baffles, twisted tape, vortex generators, and wire coil inserts. In the next section, the published papers in each field are reviewed separately. Table 1 summarizes some review papers about the potentials of different techniques for heat transfer enhancement. As presented in this table, there is no review paper to collect the research about combination of nanofluid and inserts for heat transfer enhancement.

Nanofluids and other passive techniques for heat transfer improvement

Combination of nanofluids and vortex generators for heat transfer improvement

Vortex generator can be used as a passive enhancement technique to create streamwise vortices which impose intense turbulence in fluid stream around heat transfer plates. Vortex generators disturb the flow field and disrupt the boundary layer development. Also, they create swirl flow and leads to a significant transfer of core and surface fluid, causing an improvement in heat transfer between the flow and the duct surfaces. Usually, they have four basic shapes containing delta wing (DW), delta winglet (DWP), rectangular wing (RW), and rectangular winglet (RWP). These shapes are shown in Fig. 1. Vortex generators with winglets are more suitable for improvement in heat transfer in modern thermal systems as they can create longitudinal vortices and cause disruption of the main flow field with lower values of the pressure drop [21, 22].

In 2012, Ahmed et al. [23] reviewed activities performed on heat transfer improvement by employing nanofluid or vortex generator. They did not focus on combination of both techniques. In addition, the papers published after 2012 are not reviewed in this paper. Accordingly, the papers published about combination of nanofluid and vortex generator for increasing the heat transfer rate are reviewed in this section. Ahmed et al. [23] improved numerically the heat transfer of laminar flow in a triangular channel by employing nanofluids and vortex generator (delta winglet pair). They used Al_2O_3, CuO, and SiO_2 as nanoparticles and ethylene glycol as the base fluid. They observed that the heat transfer is marginally affected by the type of nanoparticle. Accordingly, the nanoparticle of SiO_2 has the best heat transfer efficiency in comparison with other nanoparticles. Khoshvaght-Aliabadi et al. [24] carried out both experimental and numerical works to investigate the combined effects of nanofluid and vortex generator on forced convective laminar heat transfer within a plate–fin duct. They used three models containing single-phase, mixture, and Eulerian models to simulate the nanofluid. Figure 2 shows the streamlines for nanofluid flow through the duct at different values of the longitudinal pitch, for a nanoparticle volume fraction $\varphi = 0.1\%$ and a bulk Reynolds number $Re = 400$. As shown in this figure, the number of vortex generator rises by decreasing the longitudinal gap between them at a fixed duct length, and accordingly, the flow is further disturbed along the duct. Note that for larger gaps between the vortex generators, the flow downstream of the vortex generator can recover before touching the next throat, while the vicinity of the vortex generators prevents the recovering of the core flow before the next throat for smaller gaps between the vortex generators. As a result, using vortex generators with smaller longitudinal gap is more efficient and enhances more the heat transfer coefficient. Moreover, they reported that the mixture model predicts the experimental data with more accuracy in comparison with the single-phase and Eulerian models.

Ahmed and Yusoff [25] investigated the combined effects of delta winglet pair of vortex generators and nanofluids on the heat transfer and fluid flow characteristics in a triangular duct. They simulated this problem using a single-phase approach in the laminar regime. They reported that the heat transfer rate improves by increasing the attack angle in the range of 7°–30° and then decreases at 45°. Moreover, they observed that the shear stress increases by

Table 1 Some of review papers about the potentials of different techniques for heat transfer enhancement

References	Subject of review
Kakaç and Pramuanjaroenkij [11]	Potentials of nanofluids in heat transfer enhancement
Kareem et al. [13]	Potentials of corrugations in heat transfer enhancement
Sheikholeslami et al. [14]	Potentials of swirl flow equipment in heat transfer enhancement
Varun et al. [15]	Potentials of twisted tape inserts in heat transfer enhancement
Sidik et al. [16]	Potentials of passive methods for heat transfer enhancement in microchannel heat sink
Gallegos and Sharma [17]	Potentials of flexible plates as vortex generators in heat transfer enhancement
Mohammed et al. [18]	Potentials of facing step, wavy walls, and nanofluids in heat transfer enhancement

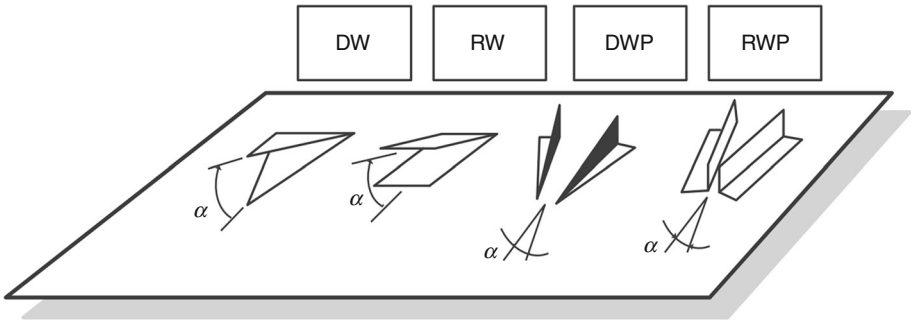

Fig. 1 Different kinds of vortex generators: delta wing (DW), rectangular wing (RW), delta winglet pair (DWP), rectangular winglet pair (RWP) reprinted from Ahmed et al. [28] with permission from Elsevier

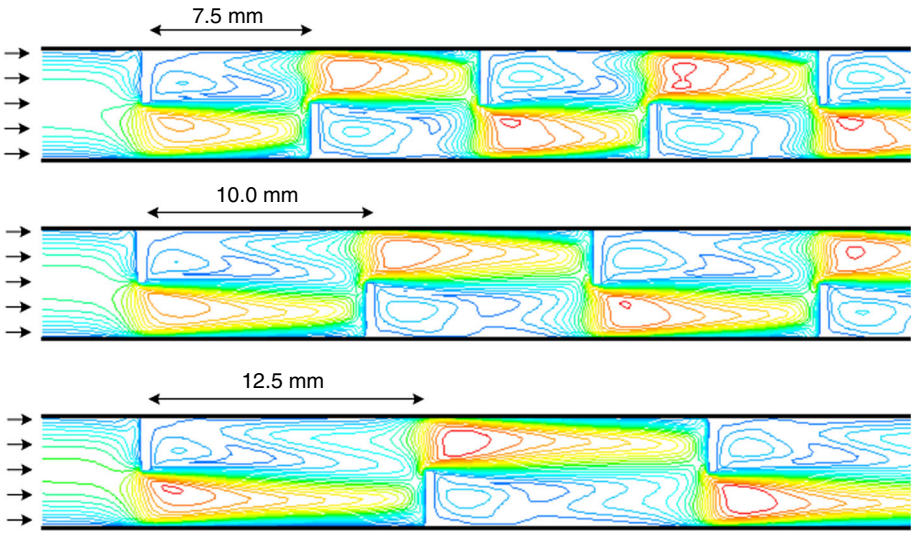

Fig. 2 Stream lines for nanofluid flow through the duct at different values of longitudinal pitch for $\varphi = 0.1\%$, and $Re = 400$ reprinted from Khoshvaght-Aliabadi et al. [24] with permission from Elsevier

increasing the attack angle or nanoparticle concentrations. In another research, Ahmed et al. [26] repeated this problem and simulated it by using a two-phase model. In this model, the nanofluid is considered as two distinct phases, while the single-phase model lumps all the effects of nanoparticles into the material parameters. They concluded that assuming the nanofluid as two distinct phases is more appropriate in comparison with considering the nanofluid as a homogeneous single-phase liquid. Abdollahi and Shams [27] optimized numerically the heat transfer improvement in nanofluid flow in a duct equipped with the winglet vortex generator. They reported that a trapezoidal vortex generator with attack angle of 51° and 0.3% concentration of nanoparticles has the highest thermohydraulic efficiency. Ahmed et al. [28] studied experimentally heat transfer improvement in a triangle duct employing combined vortex generator and nanofluid for the Reynolds number in the range of 500–8000. They reported that a good improvement in heat transfer rate by employing vortex generator in pure water, while a considerable improvement was achieved by combined employing the vortex generator and nanofluids followed with a marginal rise in the friction factor. Khoshvaght-Aliabadi [29] used experimentally the vortex generator and nanofluid in a plate–fin heat exchanger. The findings showed that the usage of vortex generator is more effective in comparison with the nanofluid on the efficiency of plate–fin heat exchangers. Khoshvaght-Aliabadi et al. [30] used experimentally Cu–water and vortex generator in a tubular heat exchanger. They used winglet vortex generator. They found that the major benefits of the vortex generators are their easy fabrication and great efficiency, especially at larger Reynolds numbers. They concluded that the nanofluid increases the pressure drop by about 8.5% for a winglets–width ratio of 0.6. Moreover, they reported a maximum PEC (performance evaluation criterion) value of 1.83. Note that the PEC can be used to take into account both heat transfer and pressure drop effects, simultaneously [31, 32]. Ebrahimi et al. [33] investigated numerically the combined influences of longitudinal vortex generators and nanofluids on the thermal performance and irreversibility in a microchannel by using a single-phase approach. They concluded that employing the nanofluids decreases the irreversibility level in the microchannel equipped with longitudinal vortex generators and, accordingly, improves the thermodynamic efficiency of the system. In another research, Sabaghan et al. [34] repeated the simulation of this problem by using a two-phase model. Their findings

indicated that the maximum normalized performance of the microchannel equipped with longitudinal vortex generator in comparison with the plain one is about 14%. Moreover, employing nanofluid can enhance the normalized performance by about 27%. Mamourian et al. [35] investigated the effects of vortex generator position on the heat transfer improvement and nanofluid homogeneity in a duct. They found that the homogeneity of the nanofluid increases as the angle of the vortex generators increases and the gap between them. Khoshvaght-Aliabadi et al. [36] evaluated experimentally the influence of changeable longitudinal spacing between delta winglet vortex generators in channels. They selected both water and Al_2O_3–water nanofluid as heat transfer fluid. They considered three arrangements for the delta winglet vortex generators as shown in Fig. 3.

They concluded that among all arrangements, the HL one exhibits the greatest heat transfer rate, while the LH arrangement has the largest pressure drop penalty. Hosseinirad and Hormozi [37] investigated numerically the influence of vortex generator shapes on the efficiencies of two coolant nanofluids in a miniature channel. These shapes were rectangular, triangular, and trapezoidal. They considered Al_2O_3–water and multiwall carbon nanotubes (MWCNT)–water-based nanofluids. Their findings indicated that Al_2O_3–water nanofluid has the largest value overall efficiency in the miniature channel with triangular vortex generator, while MWCNT–water nanofluid has the least and highest overall efficiencies in the miniature channel with triangular and trapezoidal vortex generators, respectively.

Finally, vortex generators can be used to disturb the flow field and leads to disrupt the boundary layer development. In addition, they create swirl flow and transfer a great fluid between the centre and the wall of the duct, causing an improvement in the heat transfer between the flow and the duct surfaces. Some researchers provided heat transfer rates in various thermal systems by combining this technique and nanofluid as two passive techniques. Table 2 provides the summary of researches combining vortex generators and nanofluid.

Combination of nanofluid and swirl flow device for heat transfer improvement

One of the important passive methods includes swirl flow devices that generate secondary recirculation on the axial flow causing enhancement of radial and tangential turbulent fluctuations. This leads to a superior mixing of fluid inside the domain and subsequently decreases the boundary layer thickness. Moreover, radial and tangential turbulent fluctuations generated by swirl flow devices transfer the fluid between the bulk and the near surface region. This causes different mechanisms for heat transfer improvement by enhancing flow speeds created by partial blockage of the internal flow, which decreases both hydrodynamic and thermal boundary layer thicknesses. Twisted tape and wire coil inserts are two known swirl devices. In this section, researches performed on these two devices are reviewed, separately.

Combination of nanofluids and wire coil insert for heat transfer enhancement

Some researchers combined wire coil inserts with nanofluid to achieve a higher heat transfer rate in thermal devices. Chandrasekar et al. [38] and Saeedinia et al. [39] investigated experimentally the laminar heat transfer improvement and pressure loss penalty of nanofluid flow inside a pipe equipped with wire coil inserts. Chandrasekar et al. [38] used Al_2O_3–water nanofluid, while Saeedinia et al. [39] employed CuO-based oil nanofluid. Saeedinia et al. [39] performed their experiment for Reynolds numbers in the range [10–120], while Saeedinia et al. [39] considered Reynolds numbers up to 2300. Both of these researches indicated that nanofluid has superior heat transfer efficiency as it flows through the pipes fitted by wire coil inserts in lieu of flowing through the ordinary pipe. The superior thermal efficiency of nanofluid with wire coil inserts is due to the influences of dispersion or back-mixing that increases the temperature gradient between the liquid and the surface.

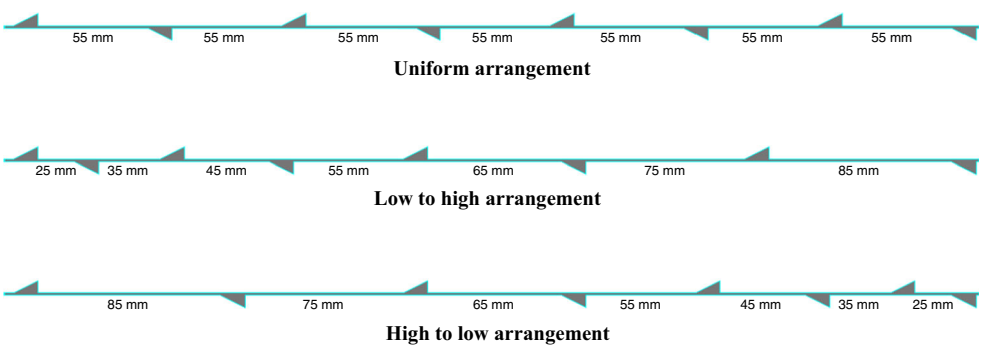

Fig. 3 Different arrangements considered for delta winglet vortex generator reprinted from Khoshvaght-Aliabadi et al. [36] with permission from Elsevier

Table 2 Researches combining vortex generators and nanofluid

References	Type of research	Type of nanofluid	Solid volume fraction/%	Particle diameter/nm	Reynolds number	Type of modelling	Type of vortex generator
Ahmed et al. [101]	Numerical	Al_2O_3, CuO, and SiO_2–ethylene glycol	1–6	25	100–800	Single-phase approach	Delta winglet pair
Khoshvaght-Aliabadi et al. [24]	Experimental/numerical	Cu–water	0, 0.1, 0.2, and 0.3	40	200–1800	Single-phase approach/two-phase mixture and Eulerian models	Rectangular wings
Ahmed and Yusoff [25]	Numerical	Al_2O_3–water	1–4	25–85	100–2000	Single-phase approach	Delta winglet pair
Abdollahi and Shams [27]	Numerical	Al_2O_3–water	0.5–3	100	250–1000	Euler–Lagrange approach	Delta winglet
Ahmed et al. [28]	Experimental	Al_2O_3 and SiO_2–water	1	25	500–8000	–	Delta winglet pair
Khoshvaght-Aliabadi et al. [30]	Experimental	Cu–water	0.2	–	5200–12,200	–	Corner delta winglets
Khoshvaght-Aliabadi [29]	Experimental	Cu–water	0.1–0.4	30–50	1850–4560	–	Rectangular wings
Ebrahimi et al. [33]	Numerical	Al_2O_3 and CuO–water	0.5–3	28.6–47	50–250	Single-phase approach	Delta winglet pair
Ahmed et al. [26]	Numerical	Al_2O_3, CuO, and SiO_2–ethylene glycol	1–4	25	100–800	Two-phase mixture model	Delta winglet pair
Sabaghan et al. [34]	Numerical	TiO_2–water	1, 1.6, and 2.3	21, 40, and 60	100–250	Two-phase mixture model	Delta winglet pair
Mamourian et al. [35]	Numerical	Al_2O_3–water	1–4	100	50–250	Euler–Lagrange approach	Rectangular shape
Hosseinirad and Hormozi [37]	Experimental/numerical	MWCNT and Al_2O_3–water	1–3	38	300–2100	Two-phase mixture model	Rectangular, trapezoidal, and triangular shapes
Khoshvaght-Aliabadi et al. [36]	Experimental	Al_2O_3–water	0.1 and 0.3	30	4000–10,000 and 100–800	–	Delta winglet

Saeedinia et al. [39] reported a maximum increment in friction factor of 22% when nanofluid with solid volume fraction of 0.3% is employed for a plain tube. An increase of 52.8% is achieved when using a coil with largest diameter for the pure oil case. In another research, Akhavan-Behabadi et al. [40] repeated this problem by using MWCNT–water nanofluid in the turbulent regime. They showed that geometrical parameters of coil wires have a significant influence on the thermal efficiency of this combined thermal system. Fallahiyekta et al. [41] investigated experimentally the turbulent heat transfer improvement in carbon nanotube (CNT)–water nanofluid flow through a pipe with wire coil inserts. They carried out their tests for Reynolds numbers between 5000 and 22,000 and concluded that wire coil inserts enhance the heat transfer rate of pure water in the pipe up to 102%. Chandrasekar et al. [42] repeated this problem by using Al_2O_3–water nanofluid in the transitional regime ($2500 \leq Re \leq 5000$). The heat transfer rate is improved by up to 34% by using the nanofluid as compared with the case of pure water for the case of the plain pipe. Kulkarni and Oak [43] used nanofluid and helical wire coil inserts to improve the heat transfer inside a tube heat exchanger. They concluded that the heat transfer rate enhances up to 140.98% by using copper oxide–water nanofluid with a solid volume fraction of 0.25% in comparison with the case of pure water. Moreover, they increase the heat transfer improvement from 140.98 to 249.45% by combining the

use of helical coil and nanofluid. For a circular tube fitted by wire coil inserts at $Re = 2290$, Chougule et al. [44] reported a heat transfer enhancement of 30.63% by employing CNT–water nanofluid with a solid volume fraction of 0.15% in comparison with the case of pure water. Moreover, they showed that the pressure loss does not increase significantly by using the nanofluid with small solid volume fraction. Mirzaei and Azimi [45] used experimentally grapheme oxide–water nanofluid and wire coil inserts to improve the heat transfer rate in a circular pipe. They showed that the heat transfer rate in this combined thermal system could be improved by up to 77% for a solid volume fraction of 0.12%. The heat transfer rate improvement also increases by increasing the volumetric flow rate of the nanofluid. Safikhani et al. [46] investigated numerically the influence of coiled wires on the thermal efficiency of nanofluids inside pipes. Their findings indicated that the heat transfer rate improves by increasing the coil diameter. They showed that the secondary flow is more intense by using a coiled wire with a larger diameter, which leads to a bigger improvement in the heat transfer rate. Goudarzi and Jamali [47] used simultaneously an Al_2O_3–ethylene glycol nanofluid and wire coil inserts to improve the heat transfer inside a car radiator. They found that the heat transfer improves by up to 9% with coil inserts. Moreover, the coupled usage of the nanofluid and the coil inserts improves the thermal efficiency by up to 5% in comparison with the case with coil inserts but without nanofluid. They showed that the thermal efficiency factor is greater than unity for all cases, which means that this combined method can be employed successfully for car radiators to enhance heat transfer rate. Sundar et al. [48] investigated nanofluid heat transfer in a pipe equipped with wire coil inserts and returned bend. They used the return bend in their system to enhance the effective liquid mixing and, accordingly, the heat transfer rate. The wire coil inserts used by Sundar et al. [48] with different values of the ratio p/d (the ratio of wire coil pitch p to inner diameter d of the pipe) are disclosed in Fig. 4. Smaller p/d ratios are beneficial for the heat transfer enhancement.

Finally, wire coils as turbulent promoters can be used to modify hydrodynamics and enhance the turbulence of the working liquid causing larger values of the heat transfer rate. They operate as artificial roughness at larger values of the Reynolds number. Their performances depend mainly on the wire coil geometry and the considered flow regime. Their main drawbacks are their very diverse persistence and reliability in regard to hot spots and corrosion effects.

Some researchers used simultaneously wire coil inserts and nanofluid to achieve larger values of the heat transfer rate. Table 3 provides the summary of researches combining these two approaches.

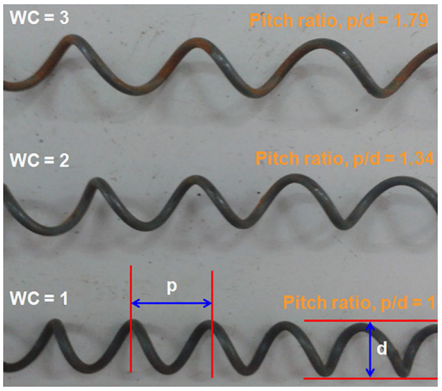

Fig. 4 Wire coil inserts reprinted from Sundar et al. [48] with permission from Elsevier

Combination of nanofluids and twisted tape inserts for heat transfer improvement

Some researchers combined twisted tape inserts with nanofluid to achieve a higher heat transfer rate in thermal systems. Sharma et al. [49] and Sundar and Sharma [50] computed the friction factor and heat transfer coefficient for a transitional nanofluid flow inside a circular pipe enhanced by twisted tape inserts. They increased the heat transfer rate by about 23.69 and 44.71% by using the nanofluid and twisted tape insert, respectively, at $Re = 9000$. Moreover, they reported that the highest friction factor with twisted tape at 0.1% nanoparticle volume fraction is 1.21 times higher than the friction factor obtained for pure water flow through a plain pipe. Pathipakka and Sivashanmugam [51] investigated numerically the combined effects of nanofluid and helical tape inserts on the laminar heat transfer in a uniformly heated circular tube. The heat transfer improvement is about 5–31% by combining these two techniques. Note that the enhancement is a function of the nanoparticle volume fraction and twist ratio. Wongcharee and Eiamsa-Ard [52] improved the heat transfer rate in a pipe by combining twisted tape with alternated axis and nanofluid. The twisted tapes with alternated axis used by Wongcharee and Eiamsa-Ard [52] are disclosed in Fig. 5. The results of previous researches confirmed that the usage of twisted tapes with alternated axis has a great heat transfer rate and thermal efficiency [53, 54]. This may be justified by the fact that the alternated axis on twisted tapes alters the flow pattern. This causes a disordered mixing between the fluid at the centre and the fluid around the pipe surface. Accordingly, this leads to a better interruption of the thermal boundary layer in comparison with the case of ordinary twisted tape, in which merely rotating flow is created. Wongcharee and Eiamsa-Ard [52] showed that twisted tape with alternated

Table 3 Research on the combination of wire coil inserts and nanofluid

References	Type of research	Type of nanoparticle	Solid volume fraction	Particle diameter	Reynolds number	Type of modelling
Chandrasekar et al. [38]	Experimental	Al_2O_3–water	0.1	43	550–2300	–
Chandrasekar et al. [42]	Experimental	Al_2O_3–water	0.1	43	2500–5000	–
Saeedinia et al. [39]	Experimental	CuO–oil	0.07–0.3	50	10–120	–
Fallahiyekta et al. [41]	Experimental	CNT-water	0.015–0.1	10–20	5000–22,000	–
Kulkarni and Oak [43]	Experimental	CuO–water	0.25	40	10,000–35,000	–
Akhavan-Behabadi et al. [40]	Experimental	MWCNT–water	0.05, 0.1, and 0.2	–	10,000–20,000	–
Mirzaei and Azimi [45]	Experimental	Graphene Oxide–water	0.02, 0.07, and 0.12	–	600–7000	–
Safikhani et al. [46]	Numerical	Al_2O_3–water	1.5 and 3	20, 40, and 100	100–500	Two-phase mixture model
Chougule et al. [44]	Experimental	MWCNT–water	0.15	10	600–2280	–
Sundar et al. [48]	Experimental	Fe_3O_4–water	0.005–0.06	–	16,000–30,000	–
Goudarzi and Jamali [47]	Experimental	Al_2O_3–ethylene glycol	0.08, 0.5 and 1	40	18,500–22,700	–

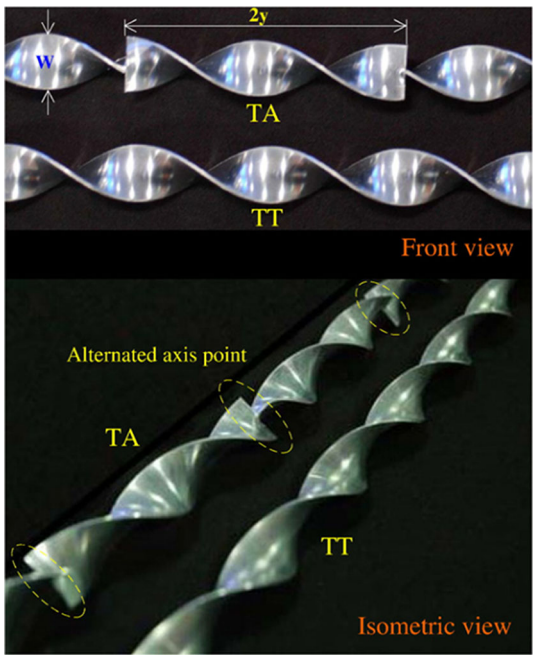

Fig. 5 Twisted tape with alternated axis reprinted from Wongcharee and Eiamsa-Ard [52] with permission from Elsevier

axis has a larger value of heat transfer (about 89%) as compared with the case of ordinary twisted tape.

Suresh et al. [55, 56] compared the thermal behaviours of the steady-state flows of aluminium oxide and copper oxide–water nanofluids inside a circular channel equipped with helical screw tape inserts displayed in Fig. 6. Note that Y represents the twist ratio (the ratio of pitch of the helical screw tape insert to the insert diameter). Their findings indicated that helical screw tape inserts have

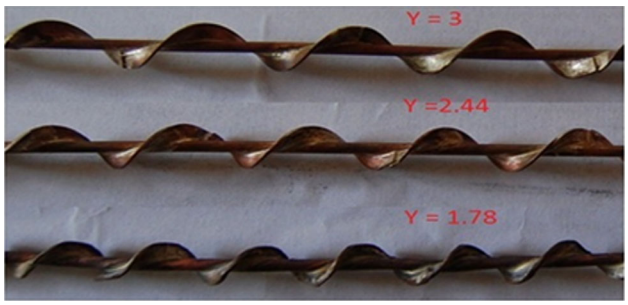

Fig. 6 Helical screw tape inserts reprinted from Suresh et al. [55] with permission from Elsevier

superior thermal efficiency as employed with copper oxide–water nanofluid.

Sundar et al. [57] investigated the combined influences of full-length twisted tape inserts and magnetic nanofluid on the turbulent flow and thermal fields in a pipe. The heat transfer rate is improved by about 30.96% by using this type of nanofluid with a volume fraction of 0.6% at $Re = 22{,}000$ for plain tube. An enhancement of 18.49% is obtained by using full-length twisted tape inserts in comparison with the plain pipe at $Re = 22{,}000$ and $\varphi = 0.6\%$. Under the same conditions, the friction factor is only 1.122 times higher. Eiamsa-Ard and Wongcharee [58] used nanofluids in a microfin pipe enhanced with single and dual twisted tapes as shown in Fig. 7. They reported that the microfin pipe enhanced by dual twisted tapes has a significantly better thermal efficiency (up to 45.4%) in comparison with one enhanced by a single tape.

Wongcharee and Eiamsa-Ard [59] improved the heat transfer in a wavy pipe by combining nanofluid and twisted

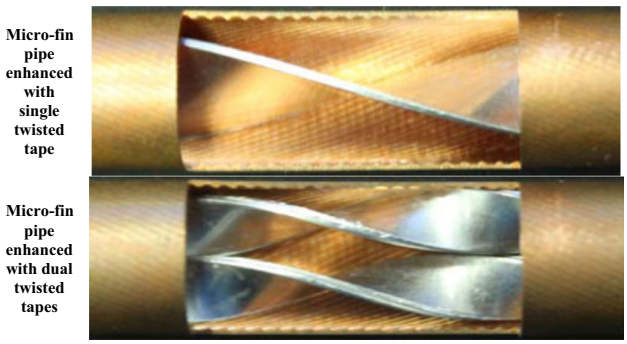

Fig. 7 Microfin pipe enhanced with single and dual twisted tapes reprinted from Eiamsa-Ard and Wongcharee [58] with permission from Elsevier

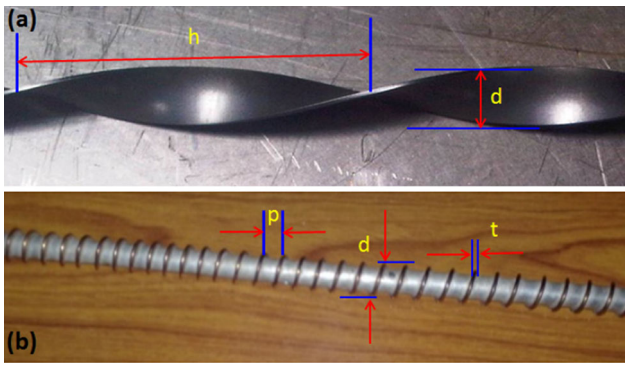

Fig. 8 **a** Twisted tape insert, **b** wire coil insert reprinted from Naik et al. [67] with permission from Elsevier

tapes. They stated that the twisted tape along the wavy pipe in counter-flow provides larger values of the thermal efficiency compared to an ordinary pipe in parallel flow. Raja Sekhar et al. [60] improved the heat transfer rate in a pipe with the combined use of nanofluid and twisted tape. Their system can be used in solar thermal systems. For a given performance level, the size of the heat exchanger can be then reduced. Moreover, they reported that this combined method is efficient as the energy achieved with heat transfer is higher in comparison with the energy lost for pumping power. Esmaeilzadeh et al. [61] studied the influences of twisted tape thickness on the thermohydraulic characteristics of the nanofluid flow within a circular pipe. They found that the heat transfer and friction increase with increasing the twisted tape thickness. Moreover, they reported that nanofluid has superior heat transfer efficiency when employed with thicker twisted strips. Maddah et al. [62] investigated experimentally the influence of twisted tape inserts and nanofluid on the heat transfer enhancement in a double pipe heat exchanger. They increased the heat transfer rate by about 25% using this combined method. Moreover, they concluded that twisted tape inserts have slightly larger values of friction factor and pressure loss as compared with the case of plain pipe without inserting the twisted tape. Salman et al. [63] used simultaneously parabolic-cut twisted tape inserts and nanofluid to improve the laminar heat transfer in a tube.

Their findings indicated that the heat transfer and friction enhance by reducing the cut depth of the twisted tape insert. This can be justified by the combined influences of usual swirling flow created by the insert and turbulence created by the intermittent cuts along the edge of the insert. This influence destructs the thermal boundary layer and generates a greater flow mixing between the fluid at the pipe centre and the fluid along the heated walls. In another research, Prasad et al. [64] used simultaneously the helical tape inserts and nanofluid inside a U-shaped tube heat exchanger. They stated that the pressure loss in the internal pass of the heat exchanger increases as the nanoparticle concentration and aspect ratio of the inserts increase. They reported a maximum value for the PEC equal to 1.13. Prasad et al. [65] used trapezoidal-cut twisted tape insert and nanofluid in a double pipe U-shaped tube heat exchanger. The findings of these studies showed that the heat transfer improvement created by combining these two techniques is higher in the tube outlet region compared to what happens at the inlet as a result of the influence of the swirl flow. Naik et al. [66, 67] investigated experimentally the thermal efficiency of the wire coil and twisted tape inserts (Fig. 8) in a tube nanofluid flow.

They reported that the thermal efficiency of nanofluid with wire coil inserts is higher in comparison with the twisted tape inserts under the same conditions. Azmi et al. [68] used experimentally TiO_2–water nanofluid in a pipe equipped with twisted tapes. They observed a maximum improvement in the heat transfer rate of 81% by using this nanofluid with a solid volume fraction of 1.0% and twisted tape insert with twist ratio of 5. In another research, Azmi et al. [69, 70] repeated this problem by comparing two nanofluids, namely TiO_2 and SiO_2–water nanofluids. They concluded that SiO_2–water nanofluid has a higher

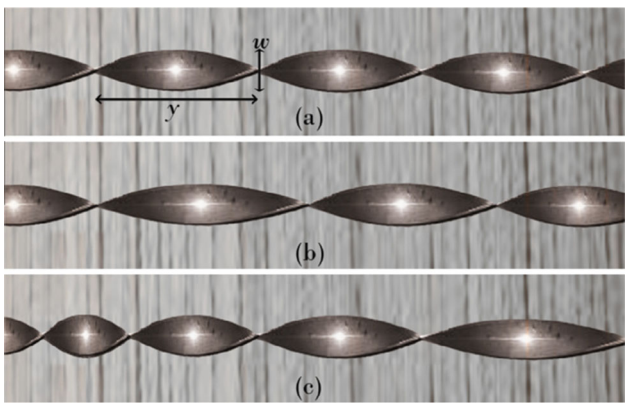

Fig. 9 Modifications on the twisted tape reprinted from Maddah et al. [72] with permission from Elsevier

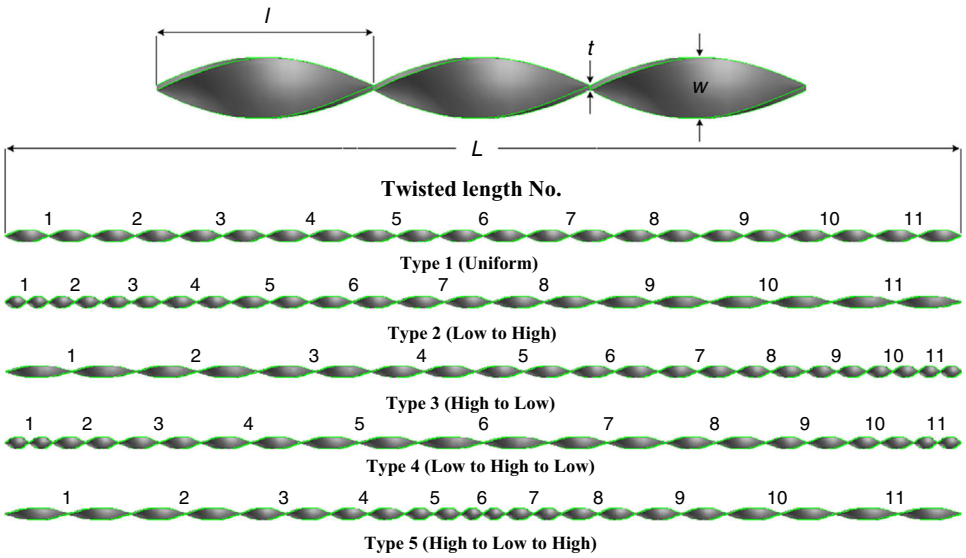

Fig. 10 Twisted tapes with different lengthes reprinted from Khoshvaght-Aliabadi and Eskandari [75] with permission from Elsevier

Procedure twist length variations (mm)											
Type no.	Twist length no.										
	1	2	3	4	5	6	7	8	9	10	11
1 (Uniform)	100	100	100	100	100	100	100	100	100	100	100
2 (L to H)	50	60	70	80	90	100	110	120	130	140	150
3 (H to L)	150	140	130	120	110	100	90	80	70	60	50
4 (L to H to L)	55	75	95	115	135	150	135	115	95	75	55
5 (H to L to H)	145	125	105	85	65	50	65	85	105	125	145

L=Low.
H=High.

heat transfer rate (about 27.9% at a solid volume fraction of 3% and twist ratio of 5) in comparison with the TiO_2 one. Eiamsa-Ard and Kiatkittipong [71] studied numerically the influence of multiple twisted tape inserts on the heat transfer improvement in nanofluid pipe flow. The heat transfer efficiency of a multiple twisted tape insert is higher in comparison with the single one. This may be justified by consecutive multiple rotating flow and multilongitudinal re-circulating flow along the pipe created by multiple twisted tape inserts. Moreover, they showed that a higher number of twisted tape inserts causes an improvement in the heat transfer efficiency, which increases the contact surface region, liquid mixing, residence time, and rotation

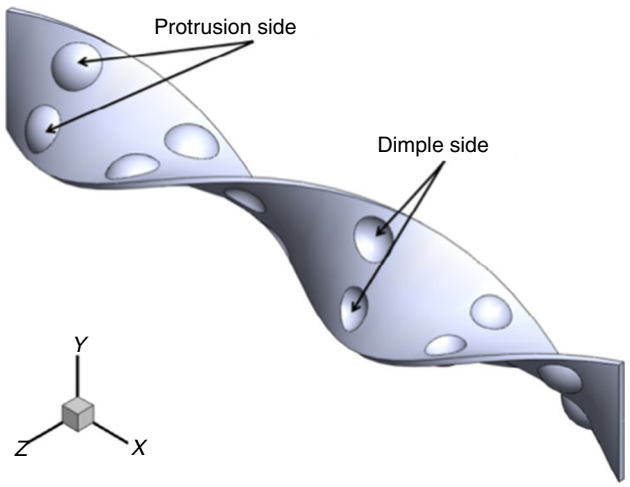

Fig. 11 Dimpled twisted tape reprinted from Zheng et al. [82] with permission from Elsevier

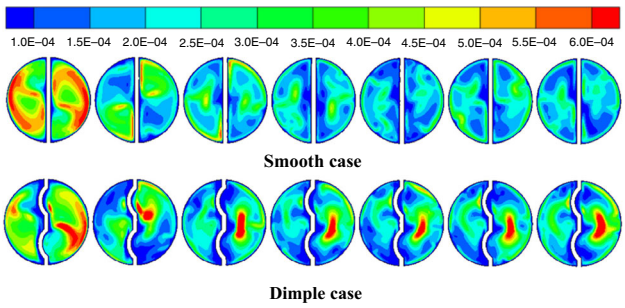

Fig. 12 Turbulence kinetic energy at different sections and $Re = 5000$ for smooth and dimple cases (flow direction is from left to right) reprinted from Zheng et al. [82] with permission from Elsevier

intensity. Maddah et al. [72] performed some modifications on the twisted tape used to improve the heat transfer in the double pipe. In their modifications, twisted tapes were both shortened and lengthened along their length. Figure 9 discloses the modifications on the twisted tapes performed by Maddah et al. [72]. Case (a) is an ordinary twisted tape, while cases (b) and (c) are modified by lengthening and shortening along the twisted tape length.

Maddah et al. [72] showed that employing a shorted twisted tape along its length coupled with nanofluid leads to maximum enhancement in the heat transfer and friction factor by about 52 and 28%, respectively, in comparison with the pipe with ordinary twisted tape coupled to nanofluid. The efficiency decreases by using a lengthened twisted tape in comparison with the pipe with an ordinary twisted one. Moreover, they concluded that PEC reduces as the Reynolds number increases. Safikhani and Eiamsa-Ard [73] used simultaneously multiple twisted tape inserts with various arrangements and nanofluid in a tube. They used the Pareto multiobjective optimization method to obtain the best condition, which means both the maximum heat transfer and the lowest pressure loss within the system. Aghayari et al. [74] studied the combined effects of perforated twisted tapes and nanofluid on the heat transfer of a double pipe heat exchanger. The twisted tapes can be fabricated with holes to decrease the pressure drop. They improved the heat transfer by about 132.2% by combining both techniques as compared with the case of pure water without inserting the twisted tape.

Khoshvaght-Aliabadi and Eskandari [75] studied experimentally the effects of twist length on the heat transfer enhancement of a nanofluid flow in a pipe. The twisted tapes with different lengths considered by Khoshvaght-Aliabadi and Eskandari [75] are shown in Fig. 10. They showed that the twist length has a significant influence on the thermo hydraulic characteristics of twisted tapes. The twisted tape of case 2 has a better thermo hydraulic efficiency compared to the other cases.

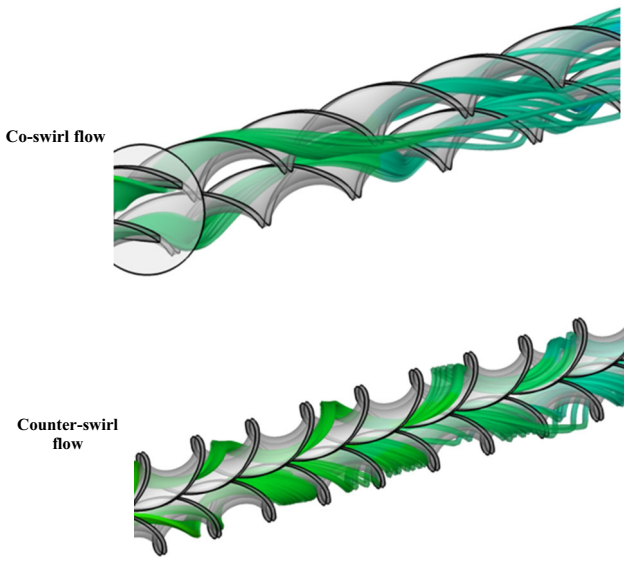

Fig. 13 Co-swirl and counter-swirl flows reprinted from Hosseinnezhad et al. [83] with permission from Springer

Safikhani and Abbasi [76] investigated numerically the nanofluid heat transfer in a flat pipe equipped with multiple twisted tapes. Indeed, they combined three heat transfer improvement techniques containing nanofluid, insert of twisted tapes, and use of flat pipes. They showed that the heat transfer improvement created by the insert of twisted tapes is higher in comparison with the two other techniques. Eiamsa-Ard et al. [77] studied both numerically and experimentally the nanofluid heat transfer in a heat exchanger pipe enhanced by an overlapped dual twisted tape. They showed that the heat transfer rate, pressure drop, and thermal efficiency increase as the overlapped twist ratio reduces or nanoparticle volume fraction increases. Chougule and Sahu [78] performed a comparison between the thermal efficiencies of Al_2O_3–water and CNT–water nanofluids flows through a tube fitted by helical screw tape inserts. They concluded that for all conditions, the CNT–water nanofluid with helical screw tape inserts has larger values of thermal efficiency in comparison with Al_2O_3–water one. They found that the Al_2O_3–water nanofluid with helical screw tape inserts has larger values of pressure drop penalty in comparison with CNT–water one. Moreover, they showed that PEC increases when decreasing the twist ratio of inserts. Sadeghi et al. [79] investigated numerically the effects of nanoparticle shapes containing cylindrical, spherical, and platelets on the heat transfer of nanofluid flow inside a circular pipe enhanced by the helical tape inserts. Their results showed that cylindrical nanoparticles have the largest heat transfer improvement and PEC among the three nanoparticle shapes considered. Prasad and Gupta [80] used simultaneously nanofluid and twisted tape inserts in a U-shaped pipe. They carried out their tests for Reynolds numbers within the range [3000; 30,000]. They reported a maximum thermal efficiency factor of 1.25 by combining the use of aluminium oxide–water nanofluid ($\varphi = 0.03\%$) and twisted tape with twist ratio of 5 in the U-shaped pipe. Buschmann [81] investigated experimentally the nanofluid laminar flow in an inserted tube with twisted tape. This research was arranged based on three distinct scaling approaches containing experiments based on the Reynolds number, the Prandtl and Reynolds numbers, and the Prandtl and Reynolds numbers and nanoparticle volume fraction. Note that the nanoparticle volume fraction is a feature of two-phase flow, which affects the thermophoretic force and Brownian motion in nanofluid flows. Buschmann [81] concluded that performing the experiment for nanofluid laminar flow in an inserted tube

Table 4 Research on the combination of twisted tapes inserts and nanofluid

References	Type of research	Type of nanofluid	Solid volume fraction	Particle diameter	Reynolds number	Type of modelling
Sharma et al. [49]	Experimental	Al_2O_3–water	0.1	47	3500–9000	–
Pathipakka and Sivashanmugam [51]	Numerical	Al_2O_3–water	0.5,1 and 1.5	30	200–2000	Single-phase approach
Sundar and Sharma [50]	Experimental	Al_2O_3–water	0.02, 0.1, and 0.5	47	10,000–22,000	–
Wongcharee and Eiamsa-Ard [52]	Experimental	CuO–water	0.3–0.7	30–50	830–1990	–
Sundar et al. [57]	Experimental	Fe_3O_4–water	0.02–0.6	36	3000–22,000	–
Wongcharee and Eiamsa-Ard [59]	Experimental	CuO–water	0.3, 0.5, and 0.7	30–50	6200–24,000	–
Eiamsa-ard and Wongcharee [58]	Experimental	CuO–water	0.3–1.0	–	5650–17,000	–
Suresh et al. [55]	Experimental	Al_2O_3 and CuO–water	0.1	Al_2O_3 (43) CuO (30)	Peclet number (5000–13,500)	–
Suresh et al. [56]	Experimental	Al_2O_3 and CuO–water	0.1	Al_2O_3 (40–50) CuO (27–37)	Peclet number (16,000–33,000)	–
Sekhar et al. [60]	Experimental	Al_2O_3–water	0.02, 0.1, and 0.5	–	800–2200	–
Naik et al. [66]	Experimental	CuO–water	0.025, 0.1, and 0.5	< 50	1000–10,000	–
Azmi et al. [68]	Experimental	TiO_2–water	0.5–3	50	8000–30,000	–
Azmi et al. [69]	Experimental–mathematical	SiO_2–water	1–4	–	3000–100,000	–
Azmi et al. [70]	Experimental	SiO_2 and TiO_2–water	1–3	SiO_2 (30) TiO_2 (50)	5000–25,000	–
Maddah et al. [62]	Experimental	TiO_2–water	0.01	30	10,000–27,500	–
Maddah et al. [72]	Experimental	Al_2O_3–water	0.3, 0.5, and 0.7	20–22	5000–21,000	–
Esmaeilzadeh et al. [61]	Experimental	γ-Al_2O_3–water	0.5–1	10–20	150–1600	–
Salman et al. [63]	Numerical	CuO–water	2 and 4	29	200–2400	Single-phase approach
Naik et al. [67]	Experimental	CuO–water	0.1 and 0.3	< 50	4000–20,000	–
Eiamsa-ard and Kiatkittipong [71]	Experimental-numerical	TiO_2–water	0.07, 0.14, and 0.21	15	5400–15,200	Single-phase approach
Prasad et al. [64]	Experimental	Al_2O_3–water	0.01–0.03	< 50	3000–30,000	–
Prasad et al. [65]	Experimental	Al_2O_3–water	0.01 and 0.03	< 50	3000–30,000	–
Eiamsa-ard et al. [77]	Experimental-numerical	TiO_2–water	0.07, 0.14, and 0.21	15	5400–15,200	Single-phase approach
Khoshvaght-Aliabadi and Eskandari [75]	Experimental	Cu–water	0.1 and 0.3	30–50	7500–15,000	–
Safikhani and Abbasi [76]	Numerical	Al_2O_3–water	3	40	100–2000	Two-phase mixture model
Aghayari et al. [74]	Experimental	Fe_2O_3–water	0.12–0.2	15	2500–20,500	–
Safikhani and Eiamsa-Ard [73]	Experimental	TiO_2–water	0. 13 and 0.21	–	5400–15,200	–
Chougule and Sahu [78]	Experimental	Al_2O_3 and CNT–water	0.15, 0.45, 0.60, and 1	Al_2O_3 (100)	2400–5600	
Prasad and Gupta [80]	Experimental	Al_2O_3–water	0.01–0.03	< 50	3000–30,000	–
Sadeghi et al. [79]	Numerical	Al_2O_3 and SiO_2–water	0.5–2.0	20–50	150–2000	Single-phase approach

Table 4 (continued)

References	Type of research	Type of nanofluid	Solid volume fraction	Particle diameter	Reynolds number	Type of modelling
Buschmann [81]	Experimental	TiO_2–water	5 and 10	30–80	300–1300	–
Zheng et al. [82]	Numerical	Al_2O_3–water	1–4	30–50	1000–10,000	Single-phase approach
Hosseinnezhad et al. [83]	Numerical	Al_2O_3–water	1–4	100	10,000–30,000	Single-phase approach
Rashidi et al. [84]	Numerical	Al_2O_3–water	1–5	60	200	Single-phase approach

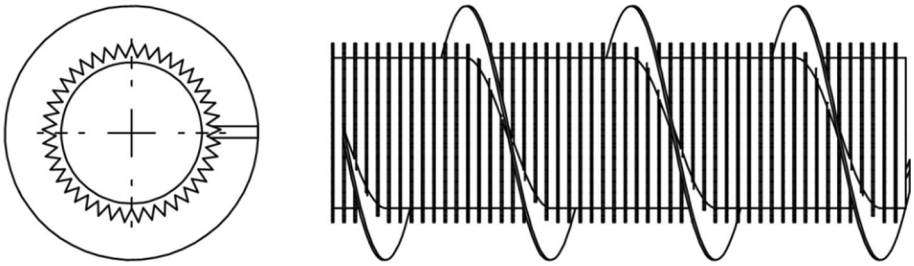

Fig. 14 Schematic of double pipe heat exchanger equipped with helical baffles reprinted from Saeedan et al. [96] with permission from Elsevier

with twisted tape based on the Prandtl and Reynolds numbers is adequate as the thermophoretic force and Brownian motion in nanofluids have less significance on this type of flow. Zheng et al. [82] investigated numerically the combined effects of dimpled twisted tapes and nanofluids on the thermal efficiency of a circular pipe. The dimpled twisted tape used by Zheng et al. [82] is displayed in Fig. 11.

Figure 12 discloses the turbulence kinetic energy (in J kg^{-1}) for the smooth and dimple cases. As shown in this figure, the turbulence kinetic energy considerably enhances particularly near the centre flow area in the case with dimples. This enhances the overall rotating flow intensity and causes more improvement in the turbulent mixing and heat transfer rate.

Hosseinnezhad et al. [83] investigated numerically the turbulent nanofluid flow through a tubular heat exchanger enhanced with twin twisted tape inserts. They considered two states for the twisted tape inserts containing co-swirl and counter-swirl flows as shown in Fig. 13. Their results indicated that the heat transfer rate enhances as the twist ratio reduces or the nanoparticle concentration increases. Moreover, they showed that the value of PEC enhancement in the counter-swirl flow state is significantly higher in comparison with the co-swirl one.

Recently, Rashidi et al. [84] numerically modelled the nanofluid flow through a square duct enhanced by a transverse twisted tap inserts. They performed both first and second laws of thermodynamic analysis. They found that the thermal (resp. viscous) irreversibility reduces (resp. increases) as the nanoparticle concentration increases or using the transverse twisted tap within the duct.

Finally, twisted or helical screw tapes can be widely employed in ducts due to their great ability to enhance the heat transfer and thermal performance. It can be justified by several reasons including a reduced hydraulic diameter, an increased length of the flow route as a result of the helical shape of this device, and an increase in the shear stress close to the duct surface, which enhances mixing. It should be pointed out that the combined usage of twisted or helical screw tapes and nanofluid has a great potential to achieve the combined advantages of improving thermal conductivity created by adding nanoparticles to base fluid and enhancing liquid mixing and growing the heat transfer length created by employing twisted or helical screw tapes. Some researchers performed various numerical and experimental works to achieve higher values of heat transfer rate by coupling these techniques. Table 4 provides the summary of researches on the combination of twisted tapes inserts and nanofluid.

Combination of nanofluids and baffles for heat transfer enhancement

Another passive technique for heat transfer improvement is to employ baffles to change the flow path. Generally, these devices shift the flow orientation and can be employed in several processes containing water cooling, clarifying, clear wells, and reservoirs water treatment equipment [85]. In thermal science, the usage of baffles interrupts both the hydraulic and thermal boundary layers and, accordingly,

causes enhancement of the heat transfer rate [86]. Indeed, the flow passing around the baffles impacts the duct surface, which can enhance the local heat transfer rate. Some researchers combined this technique with nanofluid to achieve a higher heat transfer rate in thermal devices.

Khorasanizadeh et al. [87] studied numerically nanofluid natural convection inside a cavity equipped by a conductive baffle. Their results showed that for larger values of Rayleigh number, due to the enhancement of convection, the average Nusselt number augments when one increases the concentration of nanoparticles and one relocates the baffle towards the core of the cavity. Elias et al. [88] used segmental baffles and nanofluid in a shell and tube heat exchanger. They investigated the influences of various nanoparticle shapes including cylindrical, bricks, platelets, and blades and baffle angles on the performance of this system. They stated that the cylinder-shaped nanoparticles have the best efficiency in comparison with all shapes for all baffle angles. Moreover, the 20° baffle angle has the best efficiency in comparison with other angles. Mohammed et al. [89] investigated numerically the mixed convection heat transfer of nanofluids on a backward facing step in a rectangular channel with a baffle. They found that a small displacement of the baffle leads to an intense change in the flow and temperature fields. The optimized location of the baffle insert for heat transfer improvement is related to the specific flow and thermal conditions. In another research, Heshmati et al. [90] repeated this problem for a slotted and inclined baffle. Their findings indicated that the heat transfer enhances by about 167 and 255% by combining nanofluid and a slotted baffle in comparison with employing pure water for the cases with

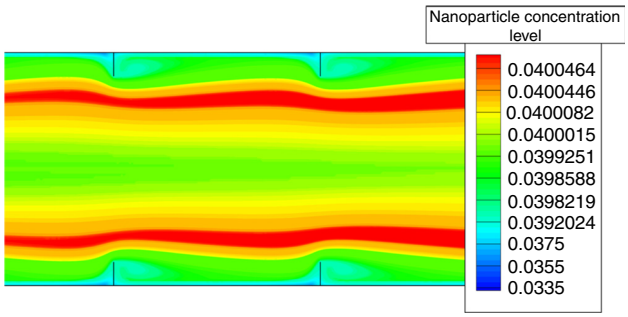

Fig. 15 Nanoparticle concentration contours between the sixth and seventh baffles at $Re = 400$, $d_p = 10$ nm, and $\varphi = 4\%$ reprinted from Fazeli et al. [97] with permission from Elsevier

Table 5 Research on the combination of baffles and nanofluid

References	Type of research	Type of nanoparticle	Solid volume fraction/%	Particle diameter/nm	Reynolds number	Type of modelling
Khorasanizadeh et al. [87]	Numerical	Cu	2–8	–	–	Single-phase approach
Elias et al. [88]	Analytical	γ-AlOOH	0.001–0.01	–	–	–
Heshmati et al. [90]	Numerical	Al_2O_3, CuO, ZnO, and SiO_2	1–4	20–50	50–100	Single-phase approach
Targui and Kahalerras [91]	Numerical	Cu, Ag, Al_2O_3 TiO_2, and CuO	2–10	–	300	Single-phase approach
Shahmohammadi and Jafari [85]	Numerical	Al_2O_3	1 and 1.6	45	600–3000	Single-phase approach and various multiphase models containing mixture, Eulerian, and volume of fluid models
Mohammed et al. [89]	Numerical	Al_2O_3, CuO, SiO_2, and ZnO	1–4	25–80	–	Single-phase approach
Bahiraei et al. [92]	Numerical	Al_2O_3	1–5	40	700–2500	Single-phase approach
Bahiraei et al. [93]	Numerical	Al_2O_3	1–5	–	–	Two-phase mixture model
Fazeli et al. [97]	Numerical	Al_2O_3	1–5	10–90	100–400	Two-phase mixture model
Saeedan et al. [96]	Numerical	Cu, CuO, and CNT	1–5	40	1000–2500	Single-phase approach
Armaghani et al. [98]	Numerical	Al_2O_3	2–6	100	1000–15,000	Single-phase approach

Table 6 Correlations of heat transfer and friction factor

References	Correlations for heat transfer and friction factor	Description
Vortex generator		
Khoshvaght-Aliabadi et al. [23]	$f = \exp(8.3670)Re^{-0.2529}(1-\varphi)^{2.0271}\left(\frac{w_h}{D_h}\right)^{4.7891}\left(\frac{w_w}{D_h}\right)^{0.8407}\left(\frac{L}{D_h}\right)^{-0.2148}\left(\frac{l_p}{D_h}\right)^{-0.1269}\left(\frac{t_p}{D_h}\right)^{-0.3925}\left(\frac{\alpha}{\beta}\right)^{0.0187}$ $\frac{Nu}{RePr^{1/3}} = \exp(-2.2957)Re^{-0.4793}(1-\varphi)^{-1.8975}\left(\frac{w_h}{D_h}\right)^{-1.6335}\left(\frac{w_w}{D_h}\right)^{0.4468}\left(\frac{L}{D_h}\right)^{-0.1197}\left(\frac{l_p}{D_h}\right)^{-1.0880}\left(\frac{t_p}{D_h}\right)^{-0.3504}\left(\frac{\alpha}{\beta}\right)^{-0.0763}$	D_h = Hydraulic diameter (m) w_h = Wing height w_w = Wing width l_p = Longitudinal pitch (m) L = Duct length (m) t_p = Transverse pitch (m) α = Wing attach angle (°) β = Wing attack angle (°) φ = Nanoparticle solid volume fraction F = Friction factor Re = Reynolds number Pr = Prandtl number
Ahmed and Yusoff [24]	$h_{ave} = -29.229 - 627.41\varphi^{378.882} + 1685.34\alpha^{0.088068}$	α = Attack angle of vortex generator (°)
Khoshvaght-Aliabadi et al. [29]	$f = 0.010Re^{-0.180}Pr^{2.511}(e_p)^{-0.241}(e_l)^{0.266}(e_w)^{0.800}$ $Nu = 0.030Re^{1.073}Pr^{-0.418}(e_p)^{-0.218}(e_l)^{0.178}(e_w)^{0.612}$	e_l = Winglets–length ratio e_p = Winglets–pitch ratio e_w = Winglets–width ratio
Khoshvaght-Aliabadi [28]	$f = 0.3586Re^{-0.150}(1-\varphi)^{-24.644}$ $Nu = 0.3141Re^{0.307}Pr^{0.705}(1-\varphi)^{-15.393}$	–
Hosseinirad and Hormozi [36]	$f_{Al_2O_3} = 5.5581Re^{-0.4723}Pr^{0.082}\left(\alpha_f \times \frac{\pi}{180}\right)^{-0.1625}\varphi^{-0.0153}$ $f_{CNT} = 1.3438Re^{-0.4575}Pr^{0.8493}\left(\alpha_f \times \frac{\pi}{180}\right)^{-0.2743}\varphi^{0.0086}$ $Nu_{Al_2O_3} = 2.3605Re^{0.5651}Pr^{0.1378}\left(\alpha_f \times \frac{\pi}{180}\right)^{-0.2085}\varphi^{0.323}$ $Nu_{CNT} = 428.076Re^{0.3124}Pr^{0.4704}\left(\alpha_f \times \frac{\pi}{180}\right)^{0.014}\varphi^{0.7212}$	α_f = Area modification factor (°)
Coil inserts		
Chandrasekar et al. [37]	$f = 530.8Re_{nf}^{-0.909}\left(\frac{p}{d}\right)^{-1.388}(1+\varphi)^{-512.26}$ $Nu = 0.279(RePr)_{nf}^{0.558}\left(\frac{p}{d}\right)^{-0.477}(1+\varphi)^{134.65}$	d = tube diameter (m) p = pitch ration nf = nanofluid
Chandrasekar et al. [41]	$f = 164.06Re_{nf}^{-0.723}\left(1+\frac{p}{d}\right)^{-1.563}(1+\varphi)^{302.09}$ $Nu = 0.0015Re_{nf}^{1.339}Pr_{nf}^{0.4}\left(1+\frac{p}{d}\right)^{-0.948}(1+\varphi)^{-37.18}$	See Chandrasekar et al. [37]

Table 6 (continued)

References	Correlations for heat transfer and friction factor	Description
Saeedinia et al. [38]	$f = 198.7Re^{-0.708}\left(\frac{p}{d}\right)^{-0.943}\left(\frac{e}{d}\right)^{0.362}\left(\frac{\mu_s}{\mu_m}\right)^{0.58}$ $Nu = 0.467Re^{0.636}Pr^{0.324}\left(\frac{p}{d}\right)^{-0.358}\left(\frac{e}{d}\right)^{0.448}\left(\frac{\mu_s}{\mu_m}\right)^{-0.14}$	μ = Dynamic viscosity (Pa s) s = Tube surface m = Bulk d = Inside diameter (m) e = Wire diameter (m) p = Wire coil pitch (m)
Fallahiyekta et al. [40]	$Nu = 1.591Re^{0.3801}Pr^{0.2865}$	–
Akhavan-Behabadi et al. [39]	$f = 0.7026Re^{-0.21}(1+\varphi)^{0.44}\left(1+\frac{p}{d}\right)^{0.02}\left(1+\frac{e}{d}\right)^{0.79}$ $Nu = 0.1763Re^{0.6837}Pr^{0.0442}(1+\varphi)^{0.6877}\left(1+\frac{p}{d}\right)^{0.0761}\left(1+\frac{e}{d}\right)^{0.8125}$	d = Tube inside diameter (m) e = Wire diameter (m) p = Perimeter of tube (m) f = Base fluid
Mirzaei and Azimi [44]	$\begin{cases} f_{nf}=0.835\varphi^{0.01}Re_{nf}^{-0.12} & Re < 2000 \\ f_{nf}=0.835\varphi^{0.01}Re_{nf}^{-0.12} & 2000 < Re < 7000 \end{cases}$ $Nu_{nf} = 0.084Re_{nf}^{0.707}Pr_{nf}^{0.385}\varphi^{0.074}\left(\frac{\mu_{nf}}{\mu_f}\right)^{0.145}$	
Sundar et al. [47]	$f = 0.2891Re^{-0.24}(1+\varphi)^{1.535}\left(1+\frac{p}{d}\right)^{0.04143}$ $Nu = 0.05650Re^{0.8}Pr^{0.4}(1+\varphi)^{2.051}\left(1+\frac{p}{d}\right)^{0.06759}$	p = Wire coil pitch (m) d = Inside diameter of the tube (m)
Sharma et al. [48]	$f = 172Re^{-0.96}(1.0+\varphi)^{2.15}\left(1.0+\frac{H}{D}\right)^{2.15}$ $Nu = 3.138\times10^{-3}(Re)(Pr)^{0.6}\left(1.0+\frac{H}{D}\right)^{0.03}(1+\varphi)^{1.22}$	H = Pitch for 180° rotation (m) D = Inner diameter of the tube (m)
Sundar and Sharma [49]	$f = 2.068Re^{-0.4330}(1.0+\varphi)^{0.01}\left(1.0+\frac{H}{D}\right)^{0.004815}$ $Nu = 0.03666Re^{0.8204}Pr^{0.4}\left(0.001+\frac{H}{D}\right)^{0.06281}(0.001+\varphi)^{0.04704}$	See Sharma et al. [48]
Twisted tapes		
Suresh et al. [54]	$f_{Al_2O_3} = 177.15(Re)^{-0.6821}\left(\frac{p}{D}\right)^{-0.7265}$ $Nu_{Al_2O_3} = 0.5419(RePr)^{0.53}\left(\frac{p}{D}\right)^{-0.594}$ $f_{CuO} = 176.92(Re)^{-0.6811}\left(\frac{p}{D}\right)^{-0.7277}$ $Nu_{CuO} = 0.5657(RePr)^{0.5337}\left(\frac{p}{D}\right)^{-0.6062}$	P = Pitch of the helical screw tape insert (m) D = Inner diameter of the tube (m)
Wongcharee and Eiamsa-Ard [51]	$f_{TA} = 4.487Re^{-0.297}(1+\varphi)^{0.101}$ $f_{TT} = 3.234Re^{-0.308}(1+\varphi)^{0.082}$ $Nu_{TA} = 0.026Re^{0.927}Pr^{0.4}(1+\varphi)^{0.128}$ $Nu_{TT} = 0.005Re^{1.062}Pr^{0.4}(1+\varphi)^{0.112}$	TA = Twisted tape with alternate axis TT = Typical twisted tape
Sundar et al. [56]	$f = 0.3490Re^{-0.25}(1+\varphi)^{0.21}\left(1+\frac{H}{D}\right)^{0.017}$ $Nu = 0.0223Re^{0.8}Pr^{0.5}(1+\varphi)^{0.54}\left(1+\frac{H}{D}\right)^{0.028}$	H = Pitch for 180° rotation (m) D = Inner diameter of the tube (m)

Table 6 (continued)

References	Correlations for heat transfer and friction factor	Description
Naik et al. [65]	$f = 24.08Re^{-0.8456}(1+\varphi)^{0.1720}$ for $1000 < Re < 2500$ $f = 0.2753Re^{-0.2279}(1+\varphi)^{0.2129}$ for $2500 < Re < 10000$ for $Nu_{\text{Reg}} = 0.1251Re^{0.5855}Pr^{0.4}(1+\varphi)^{0.3772}\left(1+\frac{H}{D}\right)^{0.05351}$	H = Pitch for 180° rotation (m) D = Inner diameter of the tube (m)
Azmi et al. [67]	$Nu = 0.27Re^{0.693}Pr_{\text{nf}}^{-0.3}\left(1+\frac{D}{H}\right)^{1.3}$	H = Helical pitch of the twisted tape (m)
Azmi et al. [69]	$Nu_{TiO_2} = 0.27Re^{0.693}Pr_{\text{nf}}^{-0.3}\left(1+\frac{D}{H}\right)^{1.3}$ SiO_2 − water $Nu_{SiO_2} = 0.073Re^{0.702}Pr_{\text{nf}}^{0.4}\left(1+\frac{D}{H}\right)^{1.3}$	See Azmi et al. [67]
Maddah et al. [71]	$f = 0.375Re^{-0.24}(1+3\pi\varphi)^{0.6}\left(1+\frac{\pi}{\text{TR}^{1.4}}\right)\text{GPR}^{-0.35}$ $Nu = 0.056Re^{0.72}Pr^{0.4}(1+\pi\varphi)^{2.75}\left(1+\frac{\pi}{2\text{TR}}\right)^{1.1}\text{GPR}^{-0.75}$	GPR = Geometrical progression ration TR = Twisted ratio
Esmaeilzadeh et al. [60]	$Nu_{x*} = 4.36 + a(x*)^{-b}e^{(c\cdot x*)}\left(0.001+\varphi^{d}\right)$ $\left(0.001+\left(\frac{t}{d}\right)^{f}\right)x* > 0.00468$	x = Axial distance $x^* = x/(D \times Re \times \text{Pr})$ t = Twisted tape thickness D = Tube diameter (m) $a = 46.39$, $b = 1.142$, $c = 12.37$, $d = 1.48$ and $f = 0.1796$
Naik et al. [66]	$f = 0.3345Re^{-0.25}(1+\varphi)^{0.19}\left(1+\frac{h}{d}\right)^{0.038}\left(1+\frac{p}{d}\right)^{0.1}$ $Nu = 0.019Re^{0.83}Pr^{0.4}(1+\varphi)^{0.39}\left(1+\frac{h}{d}\right)^{0.03}\left(1+\frac{p}{d}\right)^{0.1}$	d = Tube inner diameter (m) p = Power (W) h = Twisted tape width (m)
Eiamsa-ard and Kiatkittipong [70]	For tube fitted with single tape (ST), dual co-tapes (Co-DTs) triple co-tapes (Co-TTs), and quadruple co-tapes (Co-QTs): $f = 0.432Re^{-0.234}(1+N)^{1.272}(1+\varphi)^{0.842}$ $Nu = 0.103Re^{0.618}Pr^{0.4}(1+N)^{0.768}(1+\varphi)^{0.438}$ For tube fitted with single tape (ST), dual counter-tapes (C-DTs), quadruple counter-tapes in parallel counter-swirl flow arrangement (PC-QTs): $f = 0.459Re^{-0.234}(1+N)^{1.244}(1+\varphi)^{0.875}$ $Nu = 0.104Re^{0.618}Pr^{0.4}(1+N)^{0.789}(1+\varphi)^{0.439}$ For tube fitted with quadruple counter-tapes in cross-counter-swirl flow arrangement (CC-QTs): $f = 0.404Re^{-0.234}(1+N)^{1.266}(1+\varphi)^{0.916}$ $Nu = 0.096Re^{0.618}Pr^{0.4}(1+N)^{0.834}(1+\varphi)^{0.468}$	N = Number of tapes
Prasad et al. [63]	$f = 0.284Re^{-0.24}(1+\varphi)^{2.46}\left(1+\frac{p}{d}\right)^{0.04}$ $Nu = 0.096Re^{0.8}Pr^{0.4}(1+\varphi)^{2.86}\left(1+\frac{p}{d}\right)^{0.02}$	d = Inner diameter of the tube (m) p = Pitch of the insert (m)

Table 6 (continued)

References	Correlations for heat transfer and friction factor	Description
Eiamsa-ard et al. [76]	$f = 2.057Re^{-0.234}(y_o/y)^{-0.311}(1+\varphi)^{0.886}$	y = Pitch length of twisted tape (m)
	$Nu = 0.267Re^{0.617}Pr^{0.4}(y_o/y)^{-0.213}(1+\varphi)^{0.505}$	y_o = Overlapped pitch length of twisted tape (m)
Safikhani and Eiamsa-Ard [72]	ST, Co-DTs, Co-TTs, and Co-QTs:	See [Eiamsa-ard and Kiatkittipong [70]]
	$f = 0.437Re^{-0.233}(1+N)^{1.25}(1+\varphi)^{0.268}$	
	$Nu = 0.103Re^{0.618}Pr^{0.4}(1+N)^{0.768}(1+\varphi)^{0.438}$	
	CC-QTs:	
	$f = 0.416Re^{-0.234}(1+N)^{1.221}(1+\varphi)^{0.262}$	
	$Nu = 0.096Re^{0.618}Pr^{0.4}(1+N)^{0.834}(1+\varphi)^{0.468}$	
	ST, C-DTs, and PC-QTs:	
	$f = 0.468Re^{-0.234}(1+N)^{1.217}(1+\varphi)^{0.266}$	
	$Nu = 0.104Re^{0.618}Pr^{0.4}(1+N)^{0.789}(1+\varphi)^{0.439}$	
Prasad and Gupta [79]	$Nu = 09589Re^{0.8}Pr^{0.4}(1+\varphi)^{2.833}\left(1+\frac{H}{D}\right)^{0.01734}$	H = Helical pitch (m)
	$f = 0.3038Re^{-0.2423}(1+\varphi)^{2}\left(1+\frac{H}{D}\right)^{0.01824}$	D = Diameter (m)

baffle and without baffle, respectively. Targui and Kahalerras [91] used simultaneously porous baffles and nanofluid in a double pipe heat exchanger and investigated the effects of them on the performance of this system. Their results showed that in order to reach to the best thermal efficiencies, the nanofluid should be employed in the annular gaps attached to the porous baffles where the cold liquid is circulated. Shahmohammadi and Jafari [85] evaluated various multiphase models to simulate and study the influences of nanoparticles and baffles on the heat transfer improvement. They used both single-phase model and various multiphase models containing mixture, Eulerian, and volume of fluid models to simulate this problem for Reynolds numbers between 600 and 3000. They concluded that multiphase models are more accurate for predicting the heat transfer of nanofluids. Moreover, they showed that the baffle has a higher influence on the heat transfer improvement in comparison with the nanofluid for larger values of the Reynolds number (e.g., 2100–3000). Bahiraei et al. [92, 93] investigated numerically the combined effects of nanofluid and helical baffles on the energetic performance of a tube heat exchanger. Most of the baffles are segmental types that compress the shell-side flow for moving along a zigzag pass to improve the heat transfer rate. Employing this kind of baffles causes some critical problems containing creating dead areas in each portion between two tandem baffles, and as a result, it augments the fouling resistance. Another problem is the risk of vibration failure on the tube surface as a result of intense zigzag flow structure. Accordingly, helical baffles are introduced as a replacement for segmental types [94, 95] that almost decreases the above issues. They recommended that to obtain a great heat transfer rate and a small pressure loss, it is better to employ helical baffles with small helix angle. Moreover, a high solid volume fraction of nanoparticles can even be used without increasing too much the pressure drop. Bahiraei et al. [92] reported that the pressure drop increases by about 150% as the volume fraction increases in the range from 0 to 5%. Saeedan et al. [96] used numerically nanofluid and helical baffles in a double pipe heat exchanger. A schematic of the double pipe heat exchanger with helical baffles simulated by Saeedan et al. [96] is shown in Fig. 14.

Saeedan et al. [96] used Cu, CuO, and CNT nanoparticles and considered water as the base fluid. They concluded that increasing the nanoparticle volume fraction has the most significant influence on the heat transfer for Cu nanoparticles in comparison with CuO and CNT nanoparticles. Fazeli et al. [97] investigated numerically the combined effects of baffles and nanofluid on the forced convection in the entry area of a duct. They considered the nanoparticle migration in their simulation. Figure 15 shows the nanoparticle concentration contours between the sixth

Table 7 Correlations to compare the contributions of nanofluids and inserts on the friction factor and Nusselt number

References	Type of method	Correlations
Khoshvaght-Aliabadi et al. [29]	Nanofluid + vortex generator	$Nu_{water} = 0.029Re^{1.08}Pr^{-0.484}(e_p)^{-0.226}(e_l)^{0.179}(e_w)^{0.553}$
		$Nu_{Cu-water} = 0.03Re^{1.073}Pr^{-0.418}(e_p)^{-0.218}(e_l)^{0.178}(e_w)^{0.612}$
		$f_{water} = 0.01Re^{-0.177}Pr^{2.465}(e_p)^{-0.237}(e_l)^{0.255}(e_w)^{0.77}$
		$f_{Cu-water} = 0.01Re^{-0.18}Pr^{2.511}(e_p)^{-0.241}(e_l)^{0.266}(e_w)^{0.8}$
Naik et al. [66]	Nanofluid + twisted tape	$Nu_{water} = 0.019Re^{0.83}Pr^{0.4}\left(1+\frac{h}{d}\right)^{0.03}\left(1+\frac{p}{d}\right)^{0.1}$
		$Nu_{nanofluid} = 0.019\ Re^{0.83}Pr^{0.4}(1+\varphi)^{0.39}\left(1+\frac{h}{d}\right)^{0.03}\left(1+\frac{p}{d}\right)^{0.1}$
		$f_{water} = 0.3345Re^{-0.25}\left(1+\frac{h}{d}\right)^{0.038}\left(1+\frac{p}{d}\right)^{0.1}$
		$f_{nanofluid} = 0.3345Re^{-0.25}(1+\varphi)^{0.19}\left(1+\frac{h}{d}\right)^{0.038}\left(1+\frac{p}{d}\right)^{0.1}$
Sundar et al. [47]	Nanofluid + coil insert	$Nu_{water} = 0.05650Re^{0.8}Pr^{0.4}\left(1+\frac{p}{d}\right)^{0.06759}$
		$Nu_{nanofluid} = 0.05650Re^{0.8}Pr^{0.4}(1+\varphi)^{2.051}\left(1+\frac{p}{d}\right)^{0.06759}$
		$f_{water} = 0.2891Re^{-0.24}\left(1+\frac{p}{d}\right)^{0.04143}$
		$f_{nanofluid} = 0.2891Re^{-0.24}(1+\varphi)^{1.535}\left(1+\frac{p}{d}\right)^{0.04143}$

Table 8 Correlations for the PEC

References	Type of method	Correlation for performance
Khoshvaght-Aliabadi et al. [29]	Nanofluid + vortex generator	$PEC = 0.037Re^{0.1}Pr^{1.901}(e_p)^{-0.13}(e_l)^{0.27}(e_w)^{0.742}$
Wongcharee and Eiamsa-Ard [53]	Nanofluid + twisted tape	$PEC_{TA} = 4.487Re^{-0.297}(1+\varphi)^{0.101}$ $PEC_{TT} = 3.234Re^{-0.308}(1+\varphi)^{0.082}$

and seventh baffles at $Re = 400$, $d_p = 10$ nm and $\varphi = 4\%$. As shown in this figure, the nanoparticle volume fraction reduces near the walls due to the thermophoresis phenomenon. Note that the nanoparticles migrate from the region with higher temperature to the region with lower temperature. Accordingly, a substrate with large values of nanoparticle volume fraction appears over the baffles. They showed that the influence of the nanoparticle diameters on PEC depends mainly on the value of the nanoparticle volume fraction.

Armaghani et al. [98] studied the combined effects of nanofluid and baffles on the natural convection inside an L-shaped cavity. They found that the effects of nanofluid on the cooling cavity decrease as the baffle length increases. They reported that placing baffle in the cavity has a significant effect on flow field and it has a potential to disrupt the flow order.

Finally, usage of baffle leads to interrupt both hydrodynamic and thermal boundary layers and accordingly causes a superior heat transfer performance. The fluid, flowing around the baffles, strikes the duct surfaces, which has a capability to improve the positional heat transfer rate. Some researchers studied the simultaneous influence of baffles and nanofluid on the thermal efficiencies of different thermal systems. Table 5 provides the summary of researches on the combination of baffles and nanofluid.

Table 6 presents the correlations of heat transfer and friction factor for various inserts which are useful for engineering applications. Note that there is no correlation for the researches performed on the combined system of nanofluids and baffle. Accordingly, this should be considered for future works.

Table 7 presents some correlations to compare the contribution of nanofluids and inserts on the friction factor and Nusselt number. Cases with pure water highlight the contribution of inserts on the friction factor and Nusselt number without considering the nanofluids.

Table 8 presents the correlations for the PEC in two cases including the combination of nanofluid and vortex generator and of nanofluid with twisted tape insert.

Table 9 presents some data about the thermal conductivity and cost of various nanoparticles. As presented in this table, although some nanoparticles have a great thermal conductivity, their cost remains high, and accordingly, they are not affordable to use in thermal systems. As a result, the considered nanoparticles with high thermal conductivity and reasonable cost are suitable to be applied in real industrial applications.

Table 9 Thermal conductivity and cost of various nanoparticles reprinted from Elango et al. [102] with permission from Elsevier

S. no.	Nanopowders	Thermal conductivity/W m^{-1} K^{-1}	Quantity	Cost/Rs
1	Aluminium oxide (Al_2O_3)	40	25 g	2000
2	Zinc oxide (ZnO)	29	100 g	1500
3	Tin oxide (SnO_2)	36	25 g	1500
4	Iron oxide (Fe_2O_3)	7	25 g	1750
5	Gold nanopowder (Au)	315	1 g	35,029
6	Titanium dioxide (TiO_2)	3.5	100 g	12,359
7	Copper oxide (CuO)	76	5 g	3111
S	Carbon nanotubes	3000–6000	250 mg	19,521
9	Zirconium (IV) oxide (ZrO_2)	2	100 ml	10,611
10	Silicon nitride (Si_3N_4)	29–30	25 g	11,434
11	Boron nitride (BN)	30–33	50 g	4911
12	Aluminium nitride (AlN)	140–180	50 g	5193
13	Diamond nanopowder (C)	900	1 g	8755
14	Silver nanopowder (Ag)	424	5 g	12,917

Conclusions and recommendations for future works

Some researchers used simultaneously nanofluids and inserts to achieve further improvements in heat transfer performances of different thermal systems. This article performed a review of the literature on these researches. Inserts were baffles, twisted tape, vortex generators, and wire coil inserts. The main findings of these researches along with some recommendations for future studies are provided in this section.

Conclusions

The following findings can be drawn from this literature review:

Vortex generators A good improvement in the heat transfer rate was obtained by employing vortex generator in pure water, while a considerable improvement was achieved by employing the vortex generator and nanofluids simultaneously followed with a moderate rise of the friction factor. Generally, vortex generators with winglets are more suitable to improve the heat transfer in modern thermal devices as they have the ability to create longitudinal vortices and cause disruption of the main flow field with lower values of the pressure drop. Using vortex generators with a smaller longitudinal gap is more efficient from the heat transfer coefficient enhancement viewpoint. The main benefit of the vortex generators is their easy fabrication and great efficiency, especially at larger values of the Reynolds number. The usage of vortex generator is more effective in comparison with the nanofluid on the efficiency of plate–fin heat exchangers.

Wire coil inserts The geometrical parameters of coil wires have a significant influence on the thermal efficiency of the combined thermal system. The heat transfer rate enhances by increasing the coil diameter. Generally, the secondary vectors have higher strength by using a coiled wire with a larger diameter and this leads to more improvement in the heat transfer rate. The heat transfer enhances as the ratio of wire coil inserts (the ratio of wire coil pitch to the inner diameter of the pipe) reduces. A wire coil with sharp-edged shoe has superior heat transfer efficiency in comparison with the circular one.

Twisted strip inserts The heat transfer improvement created by combining the use of nanofluid and twisted tapes is higher at the pipe outlet (compared to what happens at the inlet) as a result of the influence of the swirl flow. The device performance can be enhanced without increasing the size of the heat exchanger. Nanofluid has superior heat transfer efficiency when employed with thicker twisted strips. The use of twisted tapes with alternated axis improves the thermal efficiency compared to the base case with twisted tapes. The microfin pipe enhanced by dual twisted tapes has a significantly better thermal efficiency compared to the case with a single tape. Generally, the twisted tapes are more efficient in comparison with the wire coils to enhance heat transfer, while the wire coils lower penalty of pressure drop in comparison with twisted tapes.

Baffles Helical baffles are introduced as a replacement for segmental types. A small displacement of the baffle leads to an intense change in the flow and temperature fields. When one wants to achieve high heat transfer rates and small pressure drops, it is better to employ helical baffles with small helix angle.

Recommendations for future studies

The following proposals are provided as a direction of future studies.

In terms of systems:

- Using these combined techniques in microscale thermal systems should be more evaluated in future studies as the demands for thermal systems with microscale sizes are increasing in chemical analysis, microfluidics, and biomedical diagnostics.
- The swirling influences created by twisted tapes are transferred from the pipe core towards the wall by using transverse or eccentric twisted tapes [1, 4]. Creation of the swirling flow adjacent to the surfaces causes greater mixing and centrifugal force in these regions, which is more efficient for enhancing the heat transfer rate. Combination of nanofluids and transverse or eccentric twisted tapes can be a good option for future studies since most of the researches in this field are performed for axial or concentric twisted tapes.
- Trapezoidal and triangular ducts have some advantages: easy to manufacture, superior compactness, affordable fabricating, superior mechanical strength, and lower friction factor [2, 99]. These ducts are widely used in solar collectors and heat exchangers. However, most of the previous studies for these combined systems are performed for circular and square ducts. More researches should be performed for trapezoidal and triangular ducts in these combined systems.
- Graphene as nanoparticle has excellent thermal, electrical, mechanical, and optical properties. Though having a prohibitive production cost, this material has good potential to enhance even more the performance of all these combined systems.
- Future researches could focus on porous inserts such as perforated inserts as they increase the effective surface for heat transfer and create a lower blockage against the flow.
- There is no correlation for the researches performed on combined system of nanofluids and baffle. Accordingly, this should be considered for future works.

From a methodological point of view:

- The careful preparation and dispersion of the nanoparticles in the base fluid is a key step for the long-term stability of a nanofluid in these combined systems. For each couple nanoparticle-based fluid, it includes the control of pH, the use of the appropriate surfactant at an optimal concentration, and a sufficient dispersion by ultrasound.
- Most of the researches for the combined system of wire coil inserts and nanofluid are experimental. More numerical researches can be performed in this area to prepare a comprehensive qualitative and quantitative evaluation that is toughly available in experimental studies. Future numerical models should include the real distribution of nanoparticles in terms of size and more physical phenomena like particle–particle interactions directly in the conservative equations (not through correlations for their thermophysical properties). Population balance model is a necessary further step towards a more realistic simulation of nanofluid flows.
- Combined usage of nanoparticle and inserts improves the heat transfer rate, but may also intensify the sedimentation of nanoparticles. Sedimentation can affect the performance of the systems, and accordingly, their long-term operation should be considered as a key parameter before recommending the use of nanoparticles for industrial applications.
- The performance of these systems should include more systematically the evolution of the four criteria recently used by Sekrani et al. [100]: the ratio C_{μ}/C_{k}, relating the dynamic viscosity and the thermal conductivity of the nanofluid, the Mouromtseff number Mo, which gathers all the relevant thermophysical properties of the nanofluid, the overall energetic efficiency η, which combines the normalized Nusselt number and pressure drop and the performance evaluation criterion (PEC), which is the ratio of heat transferred to the requiring pumping power.
- New criteria including the life cost of the systems have to be developed and integrated in combined energetic/economical optimization studies. For this purpose, the artificial neural network method coupled to a multiobjective algorithm like genetic algorithm appears to be a promising way for the design of combined systems, which could be integrated in industry.

Acknowledgements S. Poncet acknowledges the support of the NSERC chair on industrial energy efficiency funded by Hydro-Québec, Natural Resources Canada (CanmetENERGY) and Rio Tinto Alcan.

References

1. Rashidi S, Bafekr H, Masoodi R, Languri EM. EHD in thermal energy systems: a review of the applications, modelling, and experiments. J Electrost. 2017;90:1–14.
2. Amirahmadi SA, Rashidi S, Esfahani JA. Minimization of exergy losses in a trapezoidal duct with turbulator, roughness and beveled corners. Appl Therm Eng. 2016;107:533–43.
3. Bovand M, Rashidi S, Esfahani JA. Heat transfer enhancement and pressure drop penalty in porous solar heaters: numerical simulations. Sol Energy. 2016;123:145–59.

4. Rashidi S, Esfahani JA, Rashidi A. A review on the applications of porous materials in solar energy systems. Renew Sustain Energy Rev. 2017;73:1198–210.
5. Rashidi S, Bovand M, Esfahani JA. Structural optimization of nanofluid flow around an equilateral triangular obstacle. Energy. 2015;88:385–98.
6. Rashidi S, Zade NM, Esfahani JA. Thermo-fluid performance and entropy generation analysis for a new eccentric helical screw tape insert in a 3D tube. Chem Eng Process Process Intensif. 2017;117:27–37.
7. Akbarzadeh M, Rashidi S, Esfahani JA. Influences of corrugation profiles on entropy generation, heat transfer, pressure drop, and performance in a wavy channel. Appl Therm Eng. 2017;116:278–91.
8. Rashidi S, Mahian O, Languri EM. Applications of nanofluids in condensing and evaporating systems. J Therm Anal Calorim. 2017. https://doi.org/10.1007/s10973-017-6773-7.
9. Rashidi S, Akbarzadeh M, Masoodi R, Languri EM. Thermal-hydraulic and entropy generation analysis for turbulent flow inside a corrugated channel. Int J Heat Mass Transf. 2017;109:812–23.
10. Zade NM, Akar S, Rashidi S, Esfahani JA. Thermo-hydraulic analysis for a novel eccentric helical screw tape insert in a three dimensional tube. Appl Therm Eng. 2017;124:413–21.
11. Kakaç S, Pramuanjaroenkij A. Review of convective heat transfer enhancement with nanofluids. Int J Heat Mass Transf. 2009;52(13–14):3187–96.
12. Sundar LS, Singh MK. Convective heat transfer and friction factor correlations of nanofluid in a tube and with inserts: a review. Renew Sustain Energy Rev. 2013;20:23–35.
13. Kareem ZS, Jaafar MM, Lazim TM, Abdullah S, Abdulwahid AF. Passive heat transfer enhancement review in corrugation. Exp Therm Fluid Sci. 2015;68:22–38.
14. Sheikholeslami M, Gorji-Bandpy M, Ganji DD. Review of heat transfer enhancement methods: focus on passive methods using swirl flow devices. Renew Sustain Energy Rev. 2015;49:444–69.
15. Varun, Garg MO, Nautiyal H, Khurana S, Shukla MK. Heat transfer augmentation using twisted tape inserts: a review. Renew Sustain Energy Rev. 2016;63:193–225.
16. Sidik NA, Muhamad MN, Japar WM, Rasid ZA. An overview of passive techniques for heat transfer augmentation in microchannel heat sink. Int Commun Heat Mass Transf. 2017;88:74–83.
17. Gallegos RK, Sharma RN. Flags as vortex generators for heat transfer enhancement: gaps and challenges. Renew Sustain Energy Rev. 2017;76:950–62.
18. Mohammed KA, Talib AA, Nuraini AA, Ahmed KA. Review of forced convection nanofluids through corrugated facing step. Renew Sustain Energy Rev. 2017;75:234–41.
19. Cai J, Hu X, Xiao B, Zhou Y, Wei W. Recent developments on fractal-based approaches to nanofluids and nanoparticle aggregation. Int J Heat Mass Transf. 2017;105:623–37.
20. Zhang Z, Cai J, Chen F, Li H, Zhang W, Qi W. Progress in enhancement of CO_2 absorption by nanofluids: a mini review of mechanisms and current status. Renew Energy. 2018;118:527–35.
21. Chen Y, Fiebig M, Mitra NK. Conjugate heat transfer of a finned oval tube with a punched longitudinal vortex generator in form of a delta winglet—parametric investigations of the winglet. Int J Heat Mass Transf. 1998;41(23):3961–78.
22. Chompookham T, Thianpong C, Kwankaomeng S, Promvonge P. Heat transfer augmentation in a wedge-ribbed channel using winglet vortex generators. Int Commun Heat Mass Transf. 2010;37(2):163–9.
23. Ahmed HE, Mohammed HA, Yusoff MZ. An overview on heat transfer augmentation using vortex generators and nanofluids: approaches and applications. Renew Sustain Energy Rev. 2012;16:5951–93.
24. Khoshvaght-Aliabadi M, Hormozi F, Zamzamian A. Effects of geometrical parameters on performance of plate-fin heat exchanger: vortex-generator as core surface and nanofluid as working media. Appl Therm Eng. 2014;70(1):565–79.
25. Ahmed HE, Yusoff MZ. Impact of delta-winglet pair of vortex generators on the thermal and hydraulic performance of a triangular channel using Al_2O_3–water nanofluid. J Heat Transf. 2014;136(2):021901.
26. Ahmed HE, Yusoff MZ, Hawlader MN, Ahmed MI. Numerical analysis of heat transfer and nanofluid flow in a triangular duct with vortex generator: two-phase model. Heat Transf Asian Res. 2016;45(3):264–84.
27. Abdollahi A, Shams M. Optimization of heat transfer enhancement of nanofluid in a channel with winglet vortex generator. Appl Therm Eng. 2015;91:1116–26.
28. Ahmed HE, Ahmed MI, Yusoff MZ, Hawlader MN, Al-Ani H. Experimental study of heat transfer augmentation in non-circular duct using combined nanofluids and vortex generator. Int J Heat Mass Transf. 2015;90:1197–206.
29. Khoshvaght-Aliabadi M. Thermal performance of plate-fin heat exchanger using passive techniques: vortex-generator and nanofluid. Heat Mass Transf. 2016;52(4):819–28.
30. Khoshvaght-Aliabadi M, Akbari MH, Hormozi F. An empirical study on vortex-generator insert fitted in tubular heat exchangers with dilute Cu–water nanofluid flow. Chin J Chem Eng. 2016;24(6):728–36.
31. Sheikholeslami M, Ganji DD. Heat transfer improvement in a double pipe heat exchanger by means of perforated turbulators. Energy Convers Manag. 2016;127:112–23.
32. Webb RL, Eckert ER. Application of rough surfaces to heat exchanger design. Int J Heat Mass Transf. 1972;15(9):1647–58.
33. Ebrahimi A, Rikhtegar F, Sabaghan A, Roohi E. Heat transfer and entropy generation in a microchannel with longitudinal vortex generators using nanofluids. Energy. 2016;101:190–201.
34. Sabaghan A, Edalatpour M, Moghadam MC, Roohi E, Niazmand H. Nanofluid flow and heat transfer in a microchannel with longitudinal vortex generators: two-phase numerical simulation. Appl Therm Eng. 2016;100:179–89.
35. Mamourian M, Shirvan KM, Mirzakhanlari S, Rahimi AB. Vortex generators position effect on heat transfer and nanofluid homogeneity: a numerical investigation and sensitivity analysis. Appl Therm Eng. 2016;107:1233–47.
36. Khoshvaght-Aliabadi M, Baneshi Z, Khaligh SF. Analysis on performance of nanofluid-cooled vortex-generator channels with variable longitudinal spacing among delta-winglets. Appl Therm Eng. 2017;122:1–10.
37. Hosseinirad E, Hormozi F. New correlations to predict the thermal and hydraulic performance of different longitudinal pin fins as vortex generator in miniature channel: utilizing MWCNT-water and Al_2O_3–water nanofluids. Appl Therm Eng. 2017;118:199–213.
38. Chandrasekar M, Suresh S, Bose AC. Experimental studies on heat transfer and friction factor characteristics of Al_2O_3/water nanofluid in a circular pipe under laminar flow with wire coil inserts. Exp Therm Fluid Sci. 2010;34(2):122–30.
39. Saeedinia M, Akhavan-Behabadi MA, Nasr M. Experimental study on heat transfer and pressure drop of nanofluid flow in a horizontal coiled wire inserted tube under constant heat flux. Exp Therm Fluid Sci. 2012;36:158–68.
40. Akhavan-Behabadi MA, Shahidi M, Aligoodarz MR. An experimental study on heat transfer and pressure drop of

MWCNT-water nano-fluid inside horizontal coiled wire inserted tube. Int Commun Heat Mass Transf. 2015;63:62–72.
41. Fallahiyekta M, Nasr MJ, Rashidi A, Arjmand M. Convective heat transfer enhancement of CNT-water nanofluids in plain tube fitted with wire coil inserts. Iran J Chem Eng. 2014;11(2):43–55.
42. Chandrasekar M, Suresh S, Bose AC. Experimental studies on heat transfer and friction factor characteristics of Al_2O_3/water nanofluid in a circular pipe under transition flow with wire coil inserts. Heat Transf Eng. 2011;32(6):485–96.
43. Kulkarni SP, Oak SM. Heat transfer enhancement in tube in tube heat exchanger with helical wire coil inserts and CuO nanofluid. Int J Mech Eng. 2015;3:2321–6441.
44. Chougule SS, Nirgude VV, Gharge PD, Mayank M, Sahu SK. Heat transfer enhancements of low volume concentration CNT/water nanofluid and wire coil inserts in a circular tube. Energy Procedia. 2016;90:552–8.
45. Mirzaei M, Azimi A. Heat transfer and pressure drop characteristics of graphene oxide/water nanofluid in a circular tube fitted with wire coil insert. Exp Heat Transf. 2016;29(2):173–87.
46. Safikhani H, Zare Mehrjardi A, Safari M. Effect of inserting coiled wires in tubes on the fluid flow and heat transfer performance of nanofluids. Transp Phenom Nano Micro Scales. 2016;4(2):9–16.
47. Goudarzi K, Jamali H. Heat transfer enhancement of Al_2O_3-EG nanofluid in a car radiator with wire coil inserts. Appl Therm Eng. 2017;118:510–7.
48. Sundar LS, Bhramara P, Ravi Kumar NT, Singh MK. Sousa A.C.M. Experimental heat transfer, friction factor and effectiveness analysis of Fe_3O_4 nanofluid flow in a horizontal plain tube with return bend and wire coil inserts. Int. J Heat Mass Transf. 2017;109:440–53.
49. Sharma KV, Sundar LS, Sarma PK. Estimation of heat transfer coefficient and friction factor in the transition flow with low volume concentration of Al_2O_3 nanofluid flowing in a circular tube and with twisted tape insert. Int Commun Heat Mass Transf. 2009;36(5):503–7.
50. Sundar LS, Sharma KV. Turbulent heat transfer and friction factor of Al_2O_3 nanofluid in circular tube with twisted tape inserts. Int J Heat Mass Transf. 2010;53(7–8):1409–16.
51. Pathipakka G, Sivashanmugam P. Heat transfer behaviour of nanofluids in a uniformly heated circular tube fitted with helical inserts in laminar flow. Superlattices Microstruct. 2010;47(2):349–60.
52. Wongcharee K, Eiamsa-Ard S. Enhancement of heat transfer using CuO/water nanofluid and twisted tape with alternate axis. Int Commun Heat Mass Transf. 2011;38(6):742–8.
53. Eiamsa-Ard S, Promvonge P. Performance assessment in a heat exchanger tube with alternate clockwise and counter-clockwise twisted-tape inserts. Int J Heat Mass Transf. 2010;53(7–8):1364–72.
54. Wongcharee K, Eiamsa-Ard S. Friction and heat transfer characteristics of laminar swirl flow through the round tubes inserted with alternate clockwise and counter-clockwise twisted-tapes. Int Commun Heat Mass Transf. 2011;38(3):348–52.
55. Suresh S, Venkitaraj KP, Selvakumar P. Comparative study on thermal performance of helical screw tape inserts in laminar flow using Al_2O_3/water and CuO/water nanofluids. Superlattices Microstruct. 2011;49(6):608–22.
56. Suresh S, Venkitaraj KP, Selvakumar P, Chandrasekar M. A comparison of thermal characteristics of Al_2O_3/water and CuO/water nanofluids in transition flow through a straight circular duct fitted with helical screw tape inserts. Exp Therm Fluid Sci. 2012;39:37–44.
57. Sundar LS, Kumar NR, Naik MT, Sharma KV. Effect of full length twisted tape inserts on heat transfer and friction factor enhancement with Fe_3O_4 magnetic nanofluid inside a plain tube: an experimental study. Int J Heat Mass Transf. 2012;55(11–12):2761–8.
58. Eiamsa-Ard S, Wongcharee K. Single-phase heat transfer of CuO/water nanofluids in micro-fin tube equipped with dual twisted-tapes. Int Commun Heat Mass Transf. 2012;39(9):1453–9.
59. Wongcharee K, Eiamsa-Ard S. Heat transfer enhancement by using CuO/water nanofluid in corrugated tube equipped with twisted tape. Int Commun Heat Mass Transf. 2012;39(2):251–7.
60. Sekhar YR, Sharma KV, Karupparaj RT, Chiranjeevi C. Heat transfer enhancement with Al_2O_3 nanofluids and twisted tapes in a pipe for solar thermal applications. Procedia Eng. 2013;64:1474–84.
61. Esmaeilzadeh E, Almohammadi H, Nokhosteen A, Motezaker A, Omrani AN. Study on heat transfer and friction factor characteristics of γ-Al_2O_3/water through circular tube with twisted tape inserts with different thicknesses. Int J Therm Sci. 2014;82:72–83.
62. Maddah H, Aghayari R, Farokhi M, Jahanizadeh S, Ashtary K. Effect of twisted-tape turbulators and nanofluid on heat transfer in a double pipe heat exchanger. J Eng. 2014;2014:1–9.
63. Salman SD, Kadhum AA, Takriff MS, Mohamad AB. Heat transfer enhancement of laminar nanofluids flow in a circular tube fitted with parabolic-cut twisted tape inserts. Sci World J. 2014;2014:1–7.
64. Prasad PD, Gupta AV, Sreeramulu M, Sundar LS, Singh MK, Sousa AC. Experimental study of heat transfer and friction factor of Al_2O_3 nanofluid in U-tube heat exchanger with helical tape inserts. Exp Therm Fluid Sci. 2015;62:141–50.
65. Prasad PD, Gupta AV, Deepak K. Investigation of trapezoidal-cut twisted tape insert in a double pipe U-tube heat exchanger using Al_2O_3/water nanofluid. Procedia Mater Sci. 2015;10:50–63.
66. Naik MT, Janardana GR, Sundar LS. Experimental investigation of heat transfer and friction factor with water–propylene glycol based CuO nanofluid in a tube with twisted tape inserts. Int Commun Heat Mass Transf. 2013;46:13–21.
67. Naik MT, Fahad SS, Sundar LS, Singh MK. Comparative study on thermal performance of twisted tape and wire coil inserts in turbulent flow using CuO/water nanofluid. Exp Therm Fluid Sci. 2014;57:65–76.
68. Azmi WH, Sharma KV, Sarma PK, Mamat R, Anuar S. Comparison of convective heat transfer coefficient and friction factor of TiO_2 nanofluid flow in a tube with twisted tape inserts. Int J Therm Sci. 2014;81:84–93.
69. Azmi WH, Sharma KV, Sarma PK, Mamat R, Anuar S, Sundar LS. Numerical validation of experimental heat transfer coefficient with SiO_2 nanofluid flowing in a tube with twisted tape inserts. Appl Therm Eng. 2014;73(1):296–306.
70. Azmi WH, Sharma KV, Mamat R, Anuar S. Turbulent forced convection heat transfer of nanofluids with twisted tape insert in a plain tube. Energy Procedia. 2014;52:296–307.
71. Eiamsa-Ard S, Kiatkittipong K. Heat transfer enhancement by multiple twisted tape inserts and TiO_2/water nanofluid. Appl Therm Eng. 2014;70(1):896–924.
72. Maddah H, Alizadeh M, Ghasemi N, Alwi SR. Experimental study of Al_2O_3/water nanofluid turbulent heat transfer enhancement in the horizontal double pipes fitted with modified twisted tapes. Int J Heat Mass Transf. 2014;78:1042–54.
73. Safikhani HA, Eiamsa-Ard S. Multi-objective optimization of TiO_2–Water nanofluid flow in tubes fitted with multiple twisted tape inserts in different arrangement. Transp Phenom Nano Micro Scales. 2015;3(2):89–99.
74. Aghayari R, Maddah H, Arani JB, Mohammadiun Nikpanje E. An experimental investigation of heat transfer of Fe_2O_3/water

nanofluid in a double pipe heat exchanger. Int J Nano Dimens. 2015;6:517–24.
75. Khoshvaght-Aliabadi M, Eskandari M. Influence of twist length variations on thermal–hydraulic specifications of twisted-tape inserts in presence of Cu–water nanofluid. Exp Therm Fluid Sci. 2015;61:230–40.
76. Safikhani H, Abbasi F. Numerical study of nanofluid flow in flat tubes fitted with multiple twisted tapes. Adv Powder Technol. 2015;26(6):1609–17.
77. Eiamsa-Ard S, Kiatkittipong K, Jedsadaratanachai W. Heat transfer enhancement of TiO_2/water nanofluid in a heat exchanger tube equipped with overlapped dual twisted-tapes. Eng Sci Technol. 2015;18(3):336–50.
78. Chougule SS, Sahu SK. Heat transfer and friction characteristics of Al_2O_3/water and CNT/water nanofluids in transition flow using helical screw tape inserts–a comparative study. Chem Eng Process Process Intensif. 2015;88:78–88.
79. Sadeghi O, Mohammed HA, Bakhtiari-Nejad M, Wahid MA. Heat transfer and nanofluid flow characteristics through a circular tube fitted with helical tape inserts. Int Commun Heat Mass Transf. 2016;71:234–44.
80. Prasad PD, Gupta AV. Experimental investigation on enhancement of heat transfer using Al_2O_3/water nanofluid in a U-tube with twisted tape inserts. Int Commun Heat Mass Transf. 2016;75:154–61.
81. Buschmann MH. Nanofluid heat transfer in laminar pipe flow with twisted tape. Heat Transf Eng. 2017;38(2):162–76.
82. Zheng L, Xie Y, Zhang D. Numerical investigation on heat transfer performance and flow characteristics in circular tubes with dimpled twisted tapes using Al_2O_3–water nanofluid. Int J Heat Mass Transf. 2017;111:962–81.
83. Hosseinnezhad R, Akbari OA, Afrouzi HH, Biglarian M, Koveiti A, Toghraie D. Numerical study of turbulent nanofluid heat transfer in a tubular heat exchanger with twin twisted-tape inserts. J Therm Anal Calorim. 2017. https://doi.org/10.1007/s10973-017-6900-5.
84. Rashidi S, Akbarzadeh M, Karimi N, Masoodi R. Combined effects of nanofluid and transverse twisted-baffles on the flow structures, heat transfer and irreversibilities inside a square duct–a numerical study. Appl Therm Eng. 2018;130:135–48.
85. Shahmohammadi A, Jafari A. Application of different CFD multiphase models to investigate effects of baffles and nanoparticles on heat transfer enhancement. Front Chem Sci Eng. 2014;8(3):320–9.
86. Wang G, Stone K, Vanka SP. Unsteady heat transfer in baffled channels. J Heat Transf. 1996;118(3):585–91.
87. Khorasanizadeh H, Amani J, Nikfar M. Numerical investigation of Cu–water nanofluid natural convection and entropy generation within a cavity with an embedded conductive baffle. Sci Iran. 2012;19(6):1996–2003.
88. Elias MM, Shahrul IM, Mahbubul IM, Saidur R, Rahim NA. Effect of different nanoparticle shapes on shell and tube heat exchanger using different baffle angles and operated with nanofluid. Int J Heat Mass Transf. 2014;70:289–97.
89. Mohammed HA, Alawi OA, Wahid MA. Mixed convective nanofluid flow in a channel having backward-facing step with a baffle. Powder Technol. 2015;275:329–43.
90. Heshmati A, Mohammed HA, Darus AN. Mixed convection heat transfer of nanofluids over backward facing step having a slotted baffle. Appl Math Comput. 2014;240:368–86.
91. Targui N, Kahalerras H. Analysis of a double pipe heat exchanger performance by use of porous baffles and nanofluids. World Acad Sci Eng Technol Int J Mech Aerosp Ind Mechatron Manuf Eng. 2014;8:1546–51.
92. Bahiraei M, Hosseinalipour SM, Saeedan M. Prediction of Nusselt number and friction factor of water–Al_2O_3 nanofluid flow in shell-and-tube heat exchanger with helical baffles. Chem Eng Commun. 2015;202(2):260–8.
93. Bahiraei M, Hangi M, Saeedan M. A novel application for energy efficiency improvement using nanofluid in shell and tube heat exchanger equipped with helical baffles. Energy. 2015;93:2229–40.
94. Dong C, Chen YP, Wu JF. Flow and heat transfer performances of helical baffle heat exchangers with different baffle configurations. Appl Therm Eng. 2015;80:328–38.
95. Gao B, Bi Q, Nie Z, Wu J. Experimental study of effects of baffle helix angle on shell-side performance of shell-and-tube heat exchangers with discontinuous helical baffles. Exp Therm Fluid Sci. 2015;68:48–57.
96. Saeedan M, Nazar AR, Abbasi Y, Karimi R. CFD Investigation and neutral network modeling of heat transfer and pressure drop of nanofluids in double pipe helically baffled heat exchanger with a 3-D fined tube. Appl Therm Eng. 2016;100:721–9.
97. Fazeli H, Madani S, Mashaei PR. Nanofluid forced convection in entrance region of a baffled channel considering nanoparticle migration. Appl Therm Eng. 2016;106:293–306.
98. Armaghani T, Kasaeipoor A, Alavi N, Rashidi MM. Numerical investigation of water-alumina nanofluid natural convection heat transfer and entropy generation in a baffled L-shaped cavity. J Mol Liq. 2016;223:243–51.
99. Bashi M, Rashidi S, Esfahani JA. Exergy analysis for a plate-fin triangular duct enhanced by a porous material. Appl Therm Eng. 2017;110:1448–61.
100. Sekrani G, Poncet S, Proulx P. Modeling of convective turbulent heat transfer of water-based Al_2O_3 nanofluids in an uniformly heated pipe. Chem Eng Sci. 2018;176:205–19.
101. Ahmed HE, Mohammed HA, Yusoff MZ. Heat transfer enhancement of laminar nanofluids flow in a triangular duct using vortex generator. Superlattices Microstruct. 2012;52(3):398–415.
102. Elango T, Kannan A, Murugavel KK. Performance study on single basin single slope solar still with different water nanofluids. Desalination. 2015;360:45–51.